marine drugs

MDPI

Article

Novel Insights into the Nobilamide Family from a Deep-Sea *Bacillus*: Chemical Diversity, Biosynthesis and Antimicrobial Activity Towards Multidrug-Resistant Bacteria

Vincenza Casella [1,2,†], Gerardo Della Sala [1,*,†], Silvia Scarpato [1], Carmine Buonocore [1], Costanza Ragozzino [1,2], Pietro Tedesco [1], Daniela Coppola [1], Giovanni Andrea Vitale [1], Donatella de Pascale [1] and Fortunato Palma Esposito [1]

[1] Department of Ecosustainable Marine Biotechnology, Stazione Zoologica Anton Dohrn, Via A.F. Acton, 55, 80133 Naples, Italy; vincenza.casella@szn.it (V.C.); silvia.scarpato@szn.it (S.S.); carmine.buonocore@szn.it (C.B.); costanza.ragozzino@szn.it (C.R.); pietro.tedesco@szn.it (P.T.); daniela.coppola@szn.it (D.C.); giovanniandrea.vitale@unina.it (G.A.V.); donatella.depascale@szn.it (D.d.P.); fortunato.palmaesposito@szn.it (F.P.E.)

[2] Department of Chemical, Biological, Pharmaceutical and Environmental Sciences, University of Messina, Viale F. Stagno d'Alcontres, 31, 98166 Messina, Italy

* Correspondence: gerardo.dellasala@szn.it

† These authors contributed equally to this work.

Abstract: With rising concerns about antimicrobial resistance, the identification of new lead compounds to target multidrug-resistant bacteria is essential. This study employed a fast miniaturized screening to simultaneously cultivate and evaluate about 300 marine strains for biosurfactant and antibacterial activities, leading to the selection of the deep-sea *Bacillus halotolerans* BCP32. The integration of tandem mass spectrometry molecular networking and bioassay-guided fractionation unveiled this strain as a prolific factory of surfactins and nobilamides. Particularly, 84 nobilamide congeners were identified in the bacterial exometabolome, 71 of them being novel metabolites. Among these, four major compounds were isolated, including the known TL-119 and nobilamide I, as well as the two new nobilamides T1 and S1. TL-119 and nobilamide S1 exhibited potent antibiotic activity against various multidrug-resistant *Staphylococcus* strains and other Gram-positive pathogens, including the foodborne pathogen *Listeria monocytogenes*. Finally, in silico analysis of *Bacillus halotolerans* BCP32 genome revealed nobilamide biosynthesis to be directed by a previously unknown heptamodular nonribosomal peptide synthetase.

Keywords: *Bacillus*; antimicrobials; nobilamides; surfactins; MDR *Staphyloccus aureus*; *Listeria monocytogenes*; biosurfactant; NRPS; genome mining; molecular networking

Academic Editors: Bin-Gui Wang and Siwen Niu

Received: 21 December 2024
Revised: 8 January 2025
Accepted: 10 January 2025
Published: 14 January 2025

Citation: Casella, V.; Della Sala, G.; Scarpato, S.; Buonocore, C.; Ragozzino, C.; Tedesco, P.; Coppola, D.; Vitale, G.A.; de Pascale, D.; Palma Esposito, F. Novel Insights into the Nobilamide Family from a Deep-Sea *Bacillus*: Chemical Diversity, Biosynthesis and Antimicrobial Activity Towards Multidrug-Resistant Bacteria. *Mar. Drugs* **2025**, *23*, 41. https://doi.org/10.3390/md23010041

1. Introduction

During the last decades, the selective pressure caused by the overuse of antibiotics has led to the development of a new class of bacteria, defined as multidrug-resistant (MDR) bacteria. Most of them are resistant to at least three classes of antibiotics and represent a serious threat to human health [1], with the real risk of recreating the pre-antibiotic era. Recently, the World Health Organization (WHO) highlighted the issue represented by antimicrobial resistance, warning of a scary future scenario (https://www.who.int/publications/i/item/9789240093461, accessed on 12 September 2024) [2]. After the COVID-19 pandemic, this phenomenon was defined the "Silent Pandemic" [3]. MDR occurrence has prompted the search for new pharmaceutical leads. Bioprospecting of unexplored

environments, such as extreme marine habitat, has emerged as a promising strategy for the discovery of new natural products (NPs), especially those produced by microorganisms.

Marine microbial species have developed several adaptation strategies to survive extreme environmental conditions, often through the production of relevant molecules with biotechnological interest [4,5], such as antibiotics with innovative mechanisms of action [6–10] able to overcome the resistance issue. As a fact, microbial NPs represent the largest source of new antibiotic molecules, covering about two-thirds of the antibacterial therapies approved between 1980 and 2010 for human medicine [11,12].

Among relevant compounds, cell membrane-targeting molecules displaying a "detergent-like" activity represent one of the most promising NPs to prevent or reduce resistance mechanisms [13–15]. For example, daptomycin, a cyclic lipodepsipeptide produced by *Streptomyces roseosporus*, is among the last-resort antibiotics for the treatment of Gram-positive pathogens [16,17]. Depsipeptides are chemical compounds with both ester and amide bonds in their structures [18,19]. From a broader perspective, biosurfactants, including lipodepsipeptides, are bacterial membrane-disrupting biomolecules [20].

Today, there is a growing interest in microbial-derived biosurfactants, secreted molecules with the ability to reduce interfacial tension between liquids, showing eco-compatibility, cost-effectiveness, low toxicity, and better selectivity compared to synthetic surfactants [21,22]. They also exhibit antimicrobial, antiviral, and antitumor properties [23–25].

Among (marine) microorganisms, the members of *Bacillus* genus are well-known to produce a variety of novel peptides and lipopeptides, which have high potential as antimicrobials and biosurfactants [26–28]. These molecules are synthesized by biosynthetic gene clusters (BGCs), i.e., operonic genes, and can be easily predicted by the support of genomic data. In fact, they are usually produced by large multimodular enzymes, known as non-ribosomal peptide synthetases (NRPSs), which work as assembly lines to build peptides by sequential amino acid condensation [29,30]. Non-ribosomal peptides are non-essential compounds, classified as secondary metabolites, that confer advantages by inhibiting competitors and modulating symbiont interactions in challenging environments [31]. Typically, an NRPS module includes adenylation (A), peptidyl carrier protein (PCP), and condensation (C) domains, while the termination module has a thioesterase (TE) domain for releasing and/or cyclizing the peptide. Some modules also feature an epimerization (E) domain to convert amino acids from L- to D-form during synthesis, thereby introducing a mixture of L- and D-amino acids to give peptides a specific stereochemistry for selective interaction with the cellular target [32]. The identification of novel BGCs encoding new active molecules is of crucial importance in drug discovery, as it provides the tools to create sustainable sources of NPs.

The present work describes the screening of around 300 marine bacteria, leading to the identification of a deep-sea *Bacillus* sp. BCP32 with both antimicrobial and biosurfactant activity. Tandem mass spectrometry-based molecular networking analysis of the bacterial exometabolome demonstrated the production of the depsipeptide antibiotic TL-119/A-3302-B [33–36] and other known congeners reported as nobilamides [37], along with almost 70 new analogues, showing potent antimicrobial activity against drug-resistant Gram-positive pathogens. On the other hand, the high biosurfactant effect has been attributed to the secretion of a rich mixture of surfactins [27,38], well-known lipopeptides from *Bacillus* spp. which have been shown to exert significant antibacterial activity against *S. aureus*. Finally, in silico genome analysis enabled the identification of the previously unknown BGC which encodes the biosynthesis of TL-119/A-3302-B and the nobilamide family. This work emphasizes the importance of exploring marine microbial biodiversity for the discovery and production of novel clinically relevant molecules.

2. Results and Discussion

2.1. Microbial Collection Primary Screening and Selection of Bacillus sp. BCP32

Aiming to discover new antimicrobials and biosurfactants with membrane-disrupting activity, about 300 marine bacteria belonging to the Stazione Zoologica Anton Dohrn (SZN) library were screened. A miniaturized system was employed, setting up a micro-cultivation system for metabolite production in four steps, including (1) starting cultures, (2) metabolites production, (3) cell separation and (4) bioassay detection (as described in the Materials and Methods and shown in Figure 1). This method relies on the use of deep-well microplates, thereby allowing us to test a relatively high number of strains cultivated in different growth media to enhance the biosynthesis of a wide range of metabolites. The cetyltrimethylammonium bromide (CTAB) agar assay (followed by the oil-spreading assay for positive strains) and the agar well diffusion method [39] against *Staphylococcus aureus* 6538p and *Escherichia coli* ATCC 10536 were employed to detect the presence of biosurfactants and antimicrobials, respectively, in bacterial supernatants. Both pathogens were selected because they are the primary causes of nosocomial infections and are increasingly developing resistance to conventional antibiotics [40,41]. Among the 300 strains, particular attention was given to the strain *Bacillus* sp. BCP32 due to its significant potential as a biosurfactant producer in both the CTAB and oil spreading assays, and its notable inhibition halo against *S. aureus* 6538p. *Bacillus* sp. BCP32 is an extremophilic strain isolated from deep-sea sediments collected from Dohrn Canyon in the Gulf of Naples (Italy) [42].

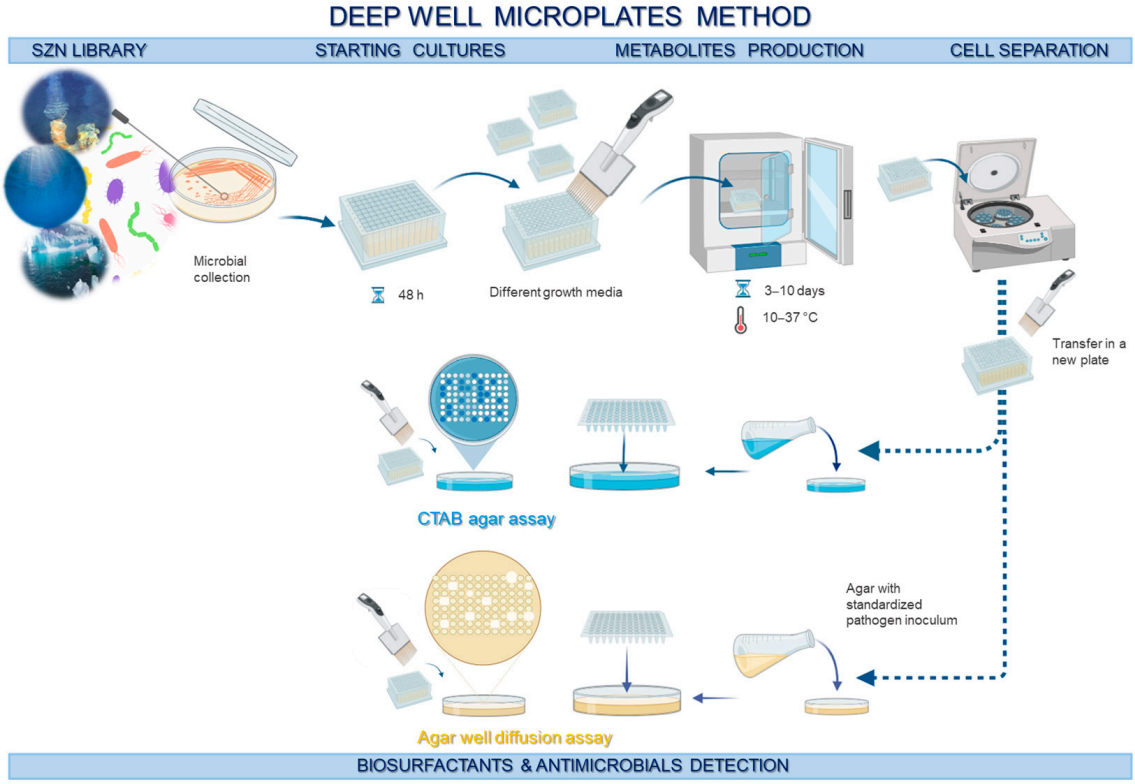

Figure 1. Graphical overview of the primary screening method applied to 300 marine bacteria from the Stazione Zoologica Anton Dohrn library. Bacterial cultures were grown in deep-well plates under various conditions, including different growth media, incubation periods, and temperatures. To evaluate their bioactivities, the CTAB agar assay was used to screen for biosurfactant production, while the agar diffusion well method was employed to assess antimicrobial activity.

2.2. Bioassay-Guided Fractionation of *Bacillus* sp. BCP32 Exhausted Broth

The selected bacterium *Bacillus* sp. BCP32 was cultivated on a small scale (50 mL in a 250 mL flask) using liquid TYP medium at 28 °C for 2 days, allowing the production of relevant metabolites to validate results from the primary screening. The exhausted broth was then extracted by ethyl acetate (EtOAc), obtaining 17 mg of crude extract, which was dissolved in DMSO (50 mg/mL) for biological assays. The oil spreading test confirmed the biosurfactant activity of *Bacillus* sp. BCP32 extract. Furthermore, the liquid inhibition assay was conducted against *S. aureus* 6538p and *E. coli* ATCC 10536, showing antibacterial activity with a MIC value of 15 µg/mL and 125 µg/mL, respectively. Based on these results, *Bacillus* sp. BCP32 was scaled-up (1L culture), and the exhausted broth was extracted by EtOAc, obtaining 430 mg of organic extract, which was fractionated by solid-phase extraction (SPE), obtaining five fractions, as described in the Section 3. Each fraction was subjected to an oil-spreading test and a liquid inhibition assay and analyzed through liquid chromatography–high-resolution tandem mass spectrometry (LC-HRMS^2). The fraction eluted with 90% MeOH (F-90% MeOH) displayed the best bioactivity in both biosurfactant and antimicrobial assays (Tables 1 and S1, Figures 2 and S1). Concerning the antibacterial activity, the pathogens panel was expanded, including several *S. aureus* MDR strains, *S. epidermidis*, *S. xylosus*, and *Listeria monocytogenes*. The F-90% MeOH showed a MIC value ranging from 0.9 µg/mL to 3.9 µg/mL (Table 1) towards all the pathogens, except for vancomycin-resistant *S. aureus* (VRSA).

Table 1. Antibacterial activity of F-90% MeOH towards a panel of Gram-positive pathogens. [a] Vancomycin, [b] erythromycin, and [c] ampicillin were used as positive controls. MIC values are expressed in µg/mL.

Strain	F-90% MeOH (MIC)	Positive Control
S. aureus 6538p	0.9	1 [a]
S. aureus 6538	0.9	0.5 [a]
S. aureus methicillin-resistant	3.9	0.5 [a]
S. aureus macrolide-resistant	3.9	0.5 [a]
S. aureus quinolone-resistant	3.9	0.5 [a]
S. aureus vancomycin-resistant	--	1 [b]
S. epidermidis RP206	1.9	0.5 [a]
S. xilosus MB5209	1.9	0.5 [a]
L. monocytogenes 677	0.9	1 [c]

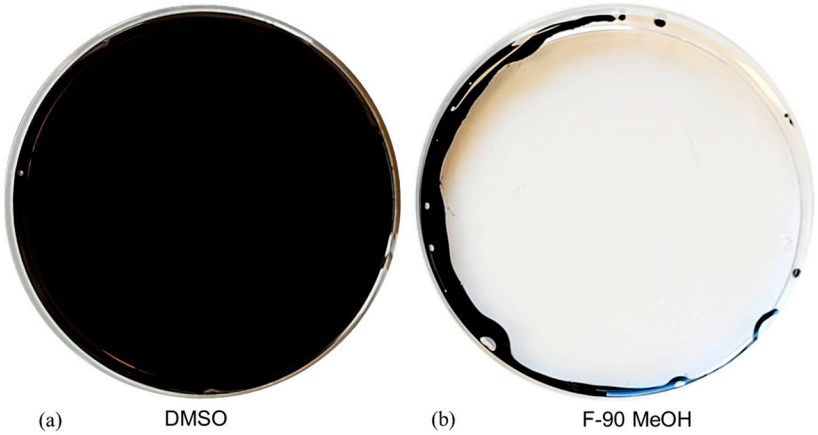

Figure 2. Surfactant activity of F-90% MeOH from *Bacillus* sp. BCP32 in the oil spreading test. (**a**) DMSO vehicle (4 µL) was used as negative control; (**b**) The clear zone on the oil surface indicates the presence of biosurfactants.

2.3. Molecular Networking Analysis of F-90% MeOH from Bacillus sp. BCP32

Since F-90% MeOH showed both biosurfactant and antimicrobial activities, the chemical space present in this fraction was mapped by feature-based molecular networking (FBMN) analysis of untargeted MS^2 data, as previously reported [43,44]. The FBMN workflow is available at the GNPS2 platform (https://gnps2.org, accessed on 2 October 2024), and generates an MS^2 spectral similarity map, highlighting structurally related molecules. The molecular network of F-90% MeOH (Figure 3) unveiled the presence of two dominant molecular clusters, including nobilamides (blue nodes) (Figure 4) and surfactins (orange nodes).

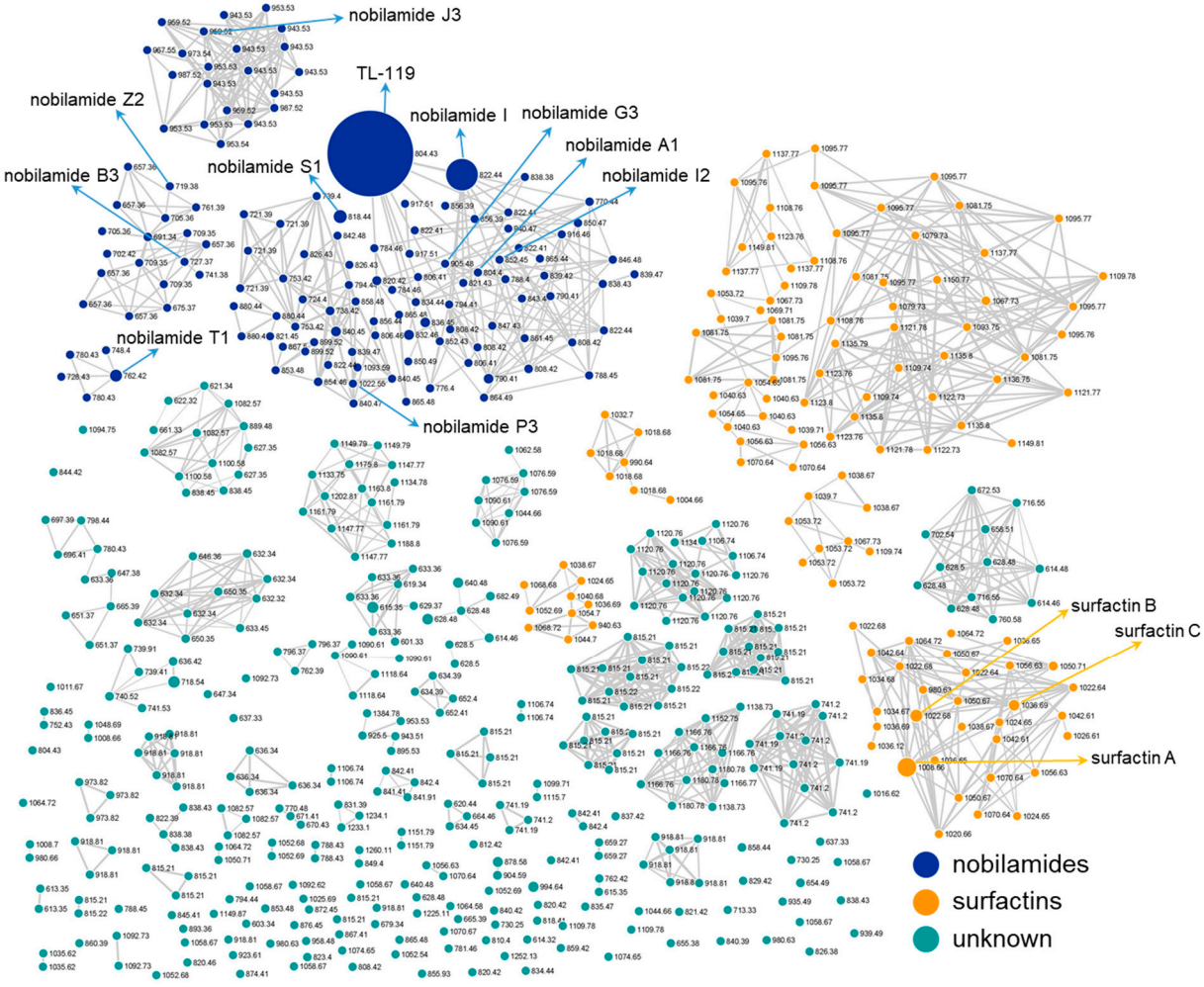

Figure 3. LC-$HRMS^2$-based molecular network (MN) of F-90% MeOH from *Bacillus* sp. BCP32. The MN is dominated by two large clusters, i.e., nobilamides (blue nodes) and surfactins (orange nodes). Compounds are visualized as nodes, and node size reflects the compound peak area. Edge thickness is related to MS^2 spectra similarity. Nobilamides reported in Figure 4 and compounds isolated in this study have been annotated in the MN.

While more than 100 nodes within the orange cluster could be promptly annotated as surfactins or surfactin analogues through the GNPS spectral library search, an in-depth manual dereplication of MS^2 data was required to identify nobilamides. As the chemical diversity of surfactins has been extensively characterized so far [45,46], we focused on the structural elucidation of nobilamides, which showed to be more effective antibiotics than surfactins (see Section 2.6). The careful examination of the product ion spectra of individual

compounds within the blue cluster allowed us to elucidate 84 nobilamide congeners, 71 of them being novel molecules.

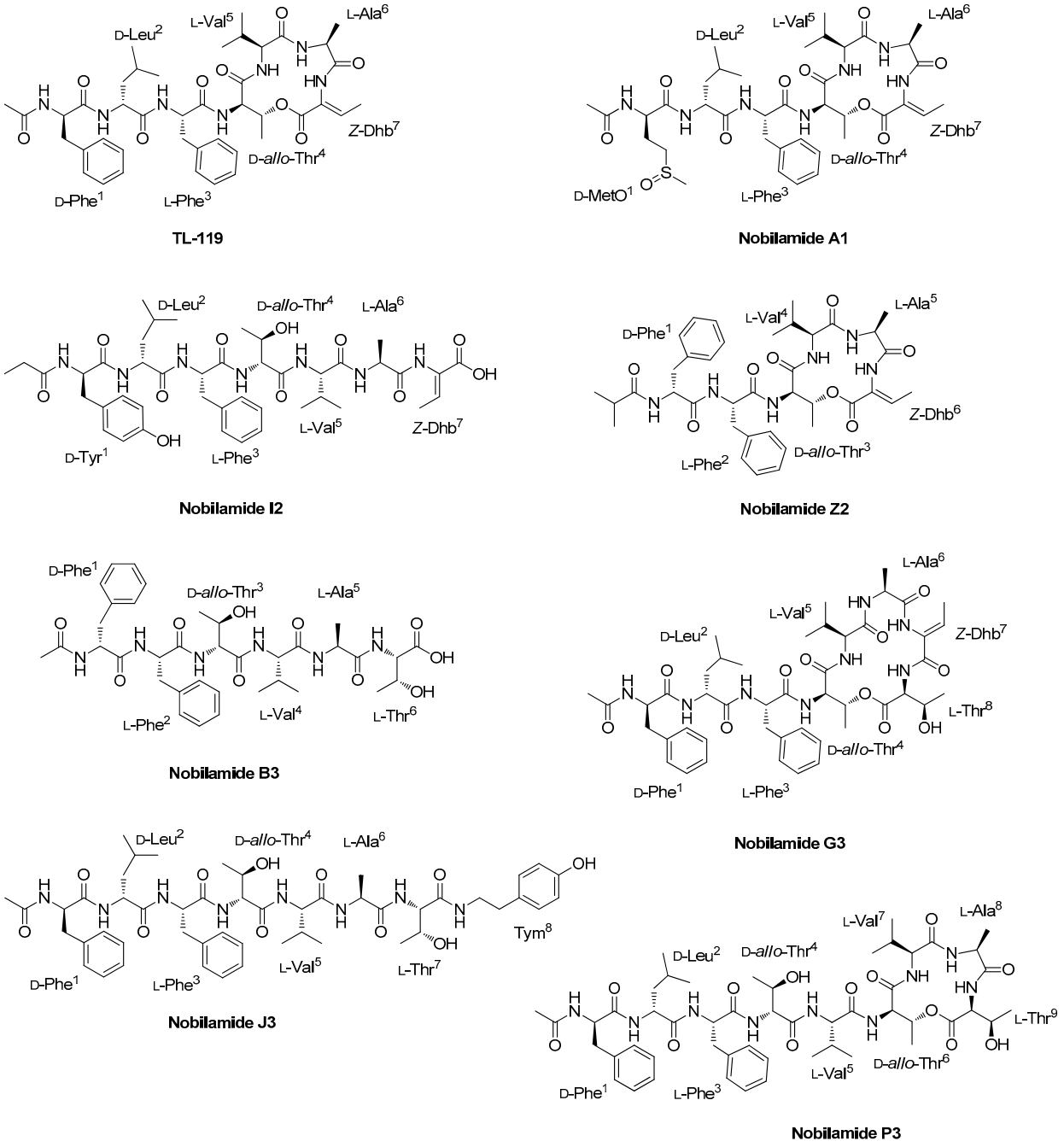

Figure 4. Chemical structures of representative nobilamides from *Bacillus* sp. BCP32.

The nobilamide family mainly comprises cyclic N-acyldepsiheptapeptides, where the D-*allo*-Thr[4] side-chain OH group forms an ester bond with the C-terminal (*Z*)-2,3-dehydrobutyrine (Figure 4). Nevertheless, nobilamides may occur also as linear heptapeptides (nobilamides A-C and S-W) [37,47]. Minor congeners, including the cyclic N-acyldepsihexapeptide nobilamide D, the linear hexapeptides nobilamide C, and the linear pentapeptide nobilamide W, have been observed in *Streptomyces* and *Bacillus* spp. [37,47]. Besides the presence of cyclic N-acyldepsiheptapeptides (32) and linear heptapeptides (26), the nobilamide cluster from *Bacillus* sp. BCP32 was shown to be composed of cyclic N-acyldepsihexapeptides (11), cyclic N-acyldepsioctapeptides (2), and cyclic N-

acyldepsinonapeptide (1), as well as linear hexapeptides (4) and octapeptides (8), thus unveiling that the nobilamide biosynthesis may take divergent paths to create an outstanding chemical diversity (Figure 4).

2.4. Structural Characterization of Nobilamide Depsiheptapeptides and Linear Heptapeptides by Mass Spectrometry and HPLC Purification

The structural characterization of the 84 nobilamide congeners was performed by LC-HRMS^2 on a Q Exactive Focus Orbitrap mass spectrometer. The high-resolution masses of the pseudomolecular ions $[M + H]^+$ included in the nobilamide network (blue nodes, Figure 3), designated the molecular formulas reported in Tables 1–7 (mass accuracy $\leq$ 3.0 ppm). Nobilamide precursor ions were selected to be fragmented in the higher-energy collision dissociation cell (HCD) and acquire MS^2 data of individual compounds (Figures S5–S83).

Table 2. Cyclic depsiheptapeptides from *Bacillus* sp. BCP32. [a] The D-*allo*-Thr/Ser^4 side-chain OH group forms an ester bond with the C-terminal residue. * Nobilamides in bold have already been reported elsewhere. Abbreviations: Ac, acetyl; Pr, propanoyl; D-*a*-Thr, D-*allo*-threonine; Dhb, 2,3-dehydrobutyrine; Dab, diaminobutyric acid.

Nobilamide *	$[M + H]^+$	*m/z*	R_t (min)	R_1	aa-1	aa-2	aa-3	aa-4 [a]	aa-5	aa-6	aa-7
X	$C_{41}H_{58}N_7O_{11}S$	856.3907	14.8	Ac	D-Phe	D-MetO	L-Phe	D-*a*-Thr	L-Val	L-Ala	L-Thr
Y	$C_{41}H_{56}N_7O_{10}S$	838.3792	16.4	Ac	D-Phe	D-MetO	L-Phe	D-*a*-Thr	L-Val	L-Ala	Z-Dhb
Z	$C_{38}H_{58}N_7O_{10}S$	804.3950	16.8	Ac	D-Phe	D-Leu	L-MetO	D-*a*-Thr	L-Val	L-Ala	Z-Dhb
A1	$C_{38}H_{58}N_7O_{10}S$	804.3950	17.2	Ac	D-MetO	D-Leu	L-Phe	D-*a*-Thr	L-Val	L-Ala	Z-Dhb
B1	$C_{42}H_{63}N_8O_{10}$	839.4654	17.7	Ac	D-Phe	D-Leu	L-Phe	D-*a*-Thr	L-Val	L-Ala	L-Dab
I	**$C_{42}H_{60}N_7O_{10}$**	**822.4387**	**19.1**	**Ac**	**D-Phe**	**D-Leu**	**L-Phe**	**D-*a*Thr**	**L-Val**	**L-Ala**	**L-Thr**
C1	$C_{41}H_{60}N_7O_9$	794.4443	19.2	-	D-Phe	D-Leu	L-Phe	D-*a*-Thr	L-Leu/Ile	L-Ala	L-Thr
N	**$C_{42}H_{58}N_7O_{10}$**	**820.4237**	**19.5**	**Ac**	**D-Phe**	**D-Leu**	**L-Phe**	**D-*a*Thr**	**L-Val**	**L-Ser**	**Z-Dhb**
D1	$C_{38}H_{58}N_7O_9S$	788.4004	20.2	Ac	D-Met	D-Leu	L-Phe	D-*a*-Thr	L-Val	L-Ala	Z-Dhb
E1	$C_{41}H_{58}N_7O_{10}$	808.4234	20.2	Ac	D-Phe	D-Leu	L-Phe	D-*a*-Thr	L-Val	L-Gly	L-Thr
F1	$C_{41}H_{56}N_7O_{10}$	806.4087	20.3	Ac	D-Phe	D-Leu	L-Phe	D-*a*-Thr	L-Thr	L-Ala	Z-Dhb
G1	$C_{38}H_{58}N_7O_9S$	788.4009	20.5	Ac	D-Phe	D-Leu	L-Met	D-*a*-Thr	L-Val	L-Ala	Z-Dhb
L	**$C_{41}H_{56}N_7O_9$**	**790.4128**	**20.6**	**Ac**	**D-Phe**	**D-Leu**	**L-Phe**	**D-*a*Thr**	**L-Val**	**L-Gly**	**Z-Dhb**
H1	$C_{42}H_{58}N_7O_{10}$	820.4236	20.7	Ac	D-Tyr	D-Leu	L-Phe	D-*a*-Thr	L-Val	L-Ala	Z-Dhb
Q	**$C_{39}H_{60}N_7O_9$**	**770.4446**	**21.2**	**Ac**	**D-Leu**	**D-Leu**	**L-Phe**	**D-*a*Thr**	**L-Val**	**L-Ala**	**Z-Dhb**
I1	$C_{40}H_{54}N_7O_9$	776.3969	21.2	Ac	D-Phe	D-Leu	L-Phe	D-*a*-Thr	L-Ala	L-Ala	Z-Dhb
J1	$C_{43}H_{60}N_7O_{10}$	834.4380	20.2	Ac	D-Phe	D-Leu	L-Phe	D-*a*-Thr	L-Val	L-Thr	Z-Dhb
O	**$C_{39}H_{60}N_7O_9$**	**770.4446**	**21.4**	**Ac**	**D-Phe**	**D-Leu**	**L-Leu**	**D-*a*Thr**	**L-Val**	**L-Ala**	**Z-Dhb**
K1	$C_{43}H_{60}N_7O_{10}$	834.4392	21.4	Pr	D-Tyr	D-Leu	L-Phe	D-*a*-Thr	L-Val	L-Ala	Z-Dhb
L1	$C_{41}H_{56}N_7O_9$	790.4133	21.7	Ac	D-Phe	D-Leu	L-Phe	D-Ser	L-Val	L-Ala	Z-Dhb
TL-119 (A-3302-B)	**$C_{42}H_{58}N_7O_9$**	**804.4289**	**22.0**	**Ac**	**D-Phe**	**D-Leu**	**L-Phe**	**D-*a*Thr**	**L-Val**	**L-Ala**	**Z-Dhb**
M1	$C_{40}H_{62}N_7O_9$	784.4608	22.6	Pr	D-Leu	D-Leu	L-Phe	D-*a*-Thr	L-Val	L-Ala	Z-Dhb
N1	$C_{40}H_{62}N_7O_9$	784.4608	22.6	Pr	D-Phe	D-Leu	L-Leu	D-*a*-Thr	L-Val	L-Ala	Z-Dhb
O1	$C_{40}H_{62}N_7O_9$	784.4608	22.6	Ac	D-Leu	D-Leu	L-Phe	D-*a*-Thr	L-Leu/Ile	L-Ala	Z-Dhb
A-3302-A	**$C_{43}H_{60}N_7O_9$**	**818.4446**	**23.5**	**Pr**	**D-Phe**	**D-Leu**	**L-Phe**	**D-*a*Thr**	**L-Val**	**L-Ala**	**Z-Dhb**
P1	$C_{39}H_{54}N_7O_8$	748.4023	24.5	-	D-Phe	D-Leu	L-Phe	D-*a*-Thr	L-Val	L-Gly	Z-Dhb
J	$C_{44}H_{62}N_7O_9$	832.4604	24.5	C_4H_7O	D-Phe	D-Leu	L-Phe	D-*a*-Thr	L-Val	L-Ala	Z-Dhb
Q1	$C_{37}H_{58}N_7O_8$	728.4339	24.6	-	D-Leu	D-Leu	L-Phe	D-*a*-Thr	L-Val	L-Ala	Z-Dhb
R1	$C_{46}H_{58}N_7O_9$	852.4289	24.8	Ac	D-Phe	D-Leu	L-Phe	D-*a*-Thr	L-Phe	L-Ala	Z-Dhb
S1	$C_{43}H_{60}N_7O_9$	818.4447	24.8	Ac	D-Phe	D-Leu	L-Phe	D-*a*-Thr	L-Leu/Ile	L-Ala	Z-Dhb
K	**$C_{45}H_{64}N_7O_9$**	**846.4763**	**25.5**	**C_5H_9O**	**D-Phe**	**D-Leu**	**L-Phe**	**D-*a*Thr**	**L-Val**	**L-Ala**	**Z-Dhb**
T1	$C_{40}H_{56}N_7O_8$	762.4182	28.3	-	D-Phe	D-Leu	L-Phe	D-*a*-Thr	L-Val	L-Ala	Z-Dhb

Table 3. Linear heptapeptides from *Bacillus* sp. BCP32. * Nobilamides in bold have been already reported elsewhere. Abbreviations: Ac, acetyl; Pr, propanoyl; D-*a*-Thr, D-*allo*-threonine; Dhb, 2,3-dehydrobutyrine; *h*-Ala, *homo*-alanine; Kyn, kynurenine; Pea, phenethylamine; Tym, tyramine; OMe, methyl ester.

Nobilamide *	$[M + H]^+$	*m/z*	R_t (min)	R_1	aa-1	aa-2	aa-3	aa-4	aa-5	aa-6	aa-7
U1	$C_{38}H_{60}N_7O_{11}S$	822.4068	15.1	Ac	D-MetO	D-Leu	L-Phe	D-*a*-Thr	L-Val	L-Ala	Z-Dhb
V1	$C_{38}H_{60}N_7O_{11}S$	822.4068	15.4	Ac	D-Phe	D-Leu	L-MetO	D-*a*-Thr	L-Val	L-Ala	Z-Dhb
W1	$C_{42}H_{62}N_7O_{12}$	856.4438	16.9	Ac	D-Phe	D-Leu	L-Tyr	D-*a*-Thr	L-Val	L-Ala	L-Thr
X1	$C_{41}H_{60}N_7O_{11}$	826.4336	17.3	Ac	D-Phe	D-Leu	L-Phe	D-*a*-Thr	L-Val	L-Gly	L-Thr
S	**$C_{42}H_{62}N_7O_{11}$**	**840.4491**	**17.4**	**Ac**	**D-Phe**	**D-Leu**	**L-Phe**	**D-*a*-Thr**	**L-Val**	**L-Ala**	**L-Thr**
Y1	$C_{40}H_{56}N_7O_{10}$	794.4071	17.7	Ac	D-Phe	D-Leu	L-Phe	D-*a*-Thr	L-Ala	L-Ala	Z-Dhb
Z1	$C_{38}H_{60}N_7O_{10}S$	806.4104	17.7	Ac	D-Met	D-Leu	L-Phe	D-*a*-Thr	L-Val	L-Ala	Z-Dhb
A2	$C_{42}H_{60}N_7O_{11}$	838.4339	18.1	Ac	D-Phe	D-Leu	L-Phe	D-*a*-Thr	L-Val	L-Ser	Z-Dhb
B2	$C_{41}H_{58}N_7O_{10}$	808.4232	18.3	Ac	D-Phe	D-Leu	L-Phe	D-*a*-Thr	L-*h*-Ala	L-Ala	Z-Dhb
A	**$C_{42}H_{60}N_7O_{10}$**	**822.4388**	**18.3**	**Ac**	**D-Phe**	**D-Leu**	**L-Phe**	**D-*a*-Thr**	**L-Val**	**L-Ala**	***Z*-Dhb**
C2	$C_{42}H_{60}N_7O_{11}$	838.4336	18.4	Ac	D-Tyr	D-Leu	L-Phe	D-*a*-Thr	L-Val	L-Ala	Z-Dhb
D2	$C_{43}H_{64}N_7O_{11}$	854.4650	18.4	Ac	D-Phe	D-Leu	L-Phe	D-*a*-Thr	L-Val	L-Ala	L-Thr-OMe
E2	$C_{39}H_{62}N_7O_{10}$	788.4544	18.6	Ac	D-Phe	D-Leu	L-Leu	D-*a*-Thr	L-Val	L-Ala	Z-Dhb
F2	$C_{43}H_{61}N_8O_{11}$	865.4446	18.7	Ac	D-Phe	D-Leu	L-Kyn	D-*a*-Thr	L-Val	L-Ala	Z-Dhb
G2	$C_{39}H_{62}N_7O_{10}$	788.4538	18.8	Ac	D-Leu	D-Leu	L-Phe	D-*a*-Thr	L-Val	L-Ala	Z-Dhb
H2	$C_{41}H_{58}N_7O_{10}$	808.4232	18.8	Ac	D-Phe	D-Leu	L-Phe	D-*a*-Thr	L-Val	L-Gly	Z-Dhb
I2	$C_{43}H_{62}N_7O_{11}$	852.4490	18.8	Pr	D-Tyr	D-Leu	L-Phe	D-*a*-Thr	L-Val	L-Ala	Z-Dhb
J2	$C_{46}H_{64}N_7O_9$	858.4751	19.4	Ac	D-Phe	D-Leu	L-Phe	D-*a*-Thr	L-Val	L-Ala	Tym
K2	$C_{43}H_{62}N_7O_{10}$	836.4543	19.5	Ac	D-Phe	D-Leu	L-Phe	D-*a*-Thr	L-Val	L-Ala	Z-Dhb-OMe
B	**$C_{43}H_{62}N_7O_{10}$**	**836.4544**	**20.0**	**Pr**	**D-Phe**	**D-Leu**	**L-Phe**	**D-*a*-Thr**	**L-Val**	**L-Ala**	***Z*-Dhb**
L2	$C_{43}H_{62}N_7O_{10}$	836.4544	20.0	Pr	D-Phe	D-Leu	L-Phe	D-Ser	L-Leu/Ile	L-Ala	Z-Dhb
M2	$C_{40}H_{58}N_7O_9$	780.4287	20.4	-	D-Phe	D-Leu	L-Phe	D-*a*-Thr	L-Val	L-Ala	Z-Dhb
N2	$C_{44}H_{64}N_7O_{10}$	850.4705	20.8	C_4H_7O	D-Phe	D-Leu	L-Phe	D-*a*-Thr	L-Val	L-Ala	Z-Dhb
O2	$C_{45}H_{66}N_7O_{10}$	864.4863	21.6	C_5H_9O	D-Phe	D-Leu	L-Phe	D-*a*-Thr	L-Val	L-Ala	Z-Dhb
P2	$C_{45}H_{66}N_7O_{10}$	864.4863	21.6	C_4H_7O	D-Phe	D-Leu	L-Phe	D-*a*-Thr	L-Leu/Ile	L-Ala	Z-Dhb
Q2	$C_{46}H_{64}N_7O_8$	842.4785	21.7	Ac	D-Phe	D-Leu	L-Phe	D-*a*-Thr	L-Val	L-Ala	Pea

Table 4. Cyclic depsihexapeptides from *Bacillus* sp. BCP32. * Nobilamides in bold have been already reported elsewhere. [a] The D-*allo*-Thr^4 side-chain OH group forms an ester bond with the C-terminal residue. [b] $[M + H + NH_3]^+$. Abbreviations: Ac, acetyl; Pr, propanoyl; D-*a*-Thr, D-*allo*-threonine; Dhb, 2,3-dehydrobutyrine.

Nobilamide *	$[M + H]^+$	*m/z*	R_t (min)	R_1	aa-1	aa-2	aa-3	aa-4	aa-5	aa-6
R2	$C_{37}H_{54}N_7O_8$ [b]	724.4009	17.4	Ac	D-Phe	D-Leu	L-Phe	D-*a*-Thr [a]	L-Val	L-Gly
S2	$C_{38}H_{53}N_6O_8$	721.3908	18.2	Ac	D-Phe	D-Leu	L-Phe	D-*a*-Thr [a]	L-Val	L-Ala
T2	$C_{39}H_{58}N_7O_8$ [b]	752.4331	18.5	Pr	D-Phe	D-Leu	L-Phe	D-*a*-Thr [a]	L-Val	L-Ala
U2	$C_{39}H_{58}N_7O_8$ [b]	752.4331	18.5	Ac	D-Phe	D-Leu	L-Phe	D-*a*-Thr [a]	L-Leu/Ile	L-Ala
D	**$C_{36}H_{47}N_6O_8$**	**691.3438**	**18.9**	**Ac**	**D-Phe**	**L-Phe**	**D-*a*-Thr [a]**	**L-Val**	**L-Ala**	***Z*-Dhb**
V2	$C_{33}H_{49}N_6O_8$	657.3594	19.3	Ac	D-Leu	L-Phe	D-*a*-Thr [a]	L-Val	L-Ala	Z-Dhb
W2	$C_{33}H_{49}N_6O_8$	657.3599	19.7	Ac	D-Phe	L-Leu	D-*a*-Thr [a]	L-Val	L-Ala	Z-Dhb
X2	$C_{37}H_{49}N_6O_8$	705.3600	19.7	Pr	D-Phe	L-Phe	D-*a*-Thr [a]	L-Val	L-Ala	Z-Dhb
Y2	$C_{37}H_{49}N_6O_8$	705.3597	19.9	Ac	D-Phe	L-Phe	D-*a*-Thr [a]	L-Leu/Ile	L-Ala	Z-Dhb
Z2	$C_{38}H_{51}N_6O_8$	719.3756	20.8	C_4H_7O	D-Phe	L-Phe	D-*a*-Thr [a]	L-Val	L-Ala	Z-Dhb
A3	$C_{40}H_{53}N_6O_9$	761.3869	23.9	$C_6H_9O_2$	D-Phe	L-Phe	D-*a*-Thr [a]	L-Val	L-Ala	Z-Dhb

Table 5. Linear hexapeptides from *Bacillus* sp. BCP32. Abbreviations: Ac, acetyl; D-*a*Thr, D-*allo*-threonine; Dhb, 2,3-dehydrobutyrine.

Nobilamide	[M + H]$^+$	*m/z*	R_t (min)	R_1	aa-1	aa-2	aa-3	aa-4	aa-5	aa-6
B3	$C_{36}H_{51}N_6O_{10}$	727.3658	15.7	Ac	D-Phe	L-Phe	D-*a*Thr	L-Val	L-Ala	L-Thr
C3	$C_{33}H_{51}N_6O_9$	675.3702	16.8	Ac	D-Leu	L-Phe	D-*a*Thr	L-Val	L-Ala	Z-Dhb
D3	$C_{36}H_{49}N_6O_9$	709.3544	16.9	Ac	D-Phe	L-Phe	D-*a*Thr	L-Val	L-Ala	Z-Dhb
E3	$C_{38}H_{53}N_6O_8$	721.3905	17.7	Ac	D-Phe	D-Leu	L-Phe	Dhb	L-Val	L-Ala

Table 6. Cyclic depsioctapeptides from *Bacillus* sp. BCP32. [a] The D-*allo*-Thr^4 side-chain OH group forms an ester bond with the C-terminal residue. Abbreviations: Ac, acetyl; D-*a*Thr, D-*allo*-threonine; Dhb, 2,3-dehydrobutyrine.

Nobilamide	[M + H]$^+$	*m/z*	R_t (min)	R_1	aa-1	aa-2	aa-3	aa-4 [a]	aa-5	aa-6	aa-7	aa-8
F3	$C_{46}H_{62}N_9O_{11}$	916.4557	18.6	Ac	D-Phe	D-Leu	L-Phe	D-*a*Thr	L-Val	L-Ala	Z-Dhb	L-dehydro-Asn
G3	$C_{46}H_{65}N_8O_{11}$	905.4762	20.8	Ac	D-Phe	D-Leu	L-Phe	D-*a*Thr	L-Val	L-Ala	Z-Dhb	L-Thr

Table 7. Linear octapeptides from *Bacillus* sp. BCP32. Abbreviations: Nob, nobilamide; Ac, acetyl; D-*a*-Thr, D-*allo*-threonine; Dhb, 2,3-dehydrobutyrine; Pea, phenethylamine; Tym, tyramine; OMe-L-Thr, L-threonine methyl ether.

Nob	[M + H]$^+$	*m/z*	R_t (min)	R_1	aa-1	aa-2	aa-3	aa-4	aa-5	aa-6	aa-7	aa-8
H3	$C_{48}H_{73}N_8O_{12}$	953.5333	18.1	Ac	D-Phe	D-Leu	L-Phe	D-*a*-Thr	L-Val	L-Ala	L-Thr	L-Leu/Ile
I3	$C_{51}H_{71}N_8O_{12}$	987.5175	18.3	Ac	D-Phe	D-Leu	L-Phe	D-*a*-Thr	L-Val	L-Ala	L-Thr	L-Phe
J3	$C_{50}H_{71}N_8O_{11}$	959.5222	19.0	Ac	D-Phe	D-Leu	L-Phe	D-*a*-Thr	L-Val	L-Ala	L-Thr	Tym
K3	$C_{45}H_{65}N_8O_{11}$	893.4757	19.6	Ac	D-Phe	D-Leu	L-Phe	D-*a*-Thr	L-Val	L-Ala	Z-Dhb	L-Ala
L3	$C_{49}H_{75}N_8O_{12}$	967.5503	21.1	Ac	D-Phe	D-Leu	L-Phe	D-*a*-Thr	L-Val	L-Ala	OMe-L-Thr	L-Leu/Ile
M3	$C_{50}H_{71}N_8O_{10}$	943.5279	22.6	Ac	D-Phe	D-Leu	L-Phe	D-*a*-Thr	L-Val	L-Ala	L-Thr	Pea
N3	$C_{51}H_{73}N_8O_{11}$	973.5398	26.4	Ac	D-Phe	D-Leu	L-Phe	D-*a*-Thr	L-Val	L-Ala	OMe-L-Thr	Tym
O3	$C_{50}H_{69}N_8O_{10}$	941.5132	28.0	Ac	D-Phe	D-Leu	L-Phe	Dhb	L-Val	L-Ala	L-Thr	Tym

During mass fragmentation, cyclic nobilamides first underwent ring opening at the ester bond, thus yielding the linear fragment α, where the Thr residue forming the lactone ring is converted into a dehydrobutyrine residue (Figures 5A and S2). Sequential N- and C-terminal cleavages of the linear fragment generated a complete *y*- and *b*-type ion series which enabled the assignment of the amino acid sequence of nobilamides. In agreement with Iloabuchi and Spiteller [47], nobilamide lactones can be fairly distinguished from their linear counterparts as featuring a diagnostic neutral loss of the dehydrobutyrine residue (C_4H_5NO, 83.0371 amu) from the corresponding *b* fragment ion (e.g., b_4 ion in *N*-acyldepsiheptapeptides) (Figure 5A,B). In addition, while in most cases linear nobilamides underwent a rearrangement reaction, leading to the loss of the C-terminal residue and formation of a b_{n-1} + H_2O ion [48], nobilamide lactones gave only the b_{n-1} fragment ion, losing an intact C-terminal amino acid after the ester bond cleavage. The b_2 fragment ions of *N*-acylated nobilamides displayed neutral loss of the fatty acyl chain as ketene, which was useful to infer the acyl group linked to the N-terminal amino acid (Figure 5A).

The consensus sequences of cyclic *N*-acyldepsiheptapeptides and linear heptapeptides from *Bacillus* sp. BCP32 is D-Phe^1-D-Leu^2-L-Phe^3-D-*allo*-Thr^4-L-Val^5-L-Ala^6-(*Z*)-2,3-dehydrobutyrine^7 (Tables 2 and 3) and nicely matches the specificity prediction of A domains in the nobilamide (*nbl*) synthetase (see Section 2.7).

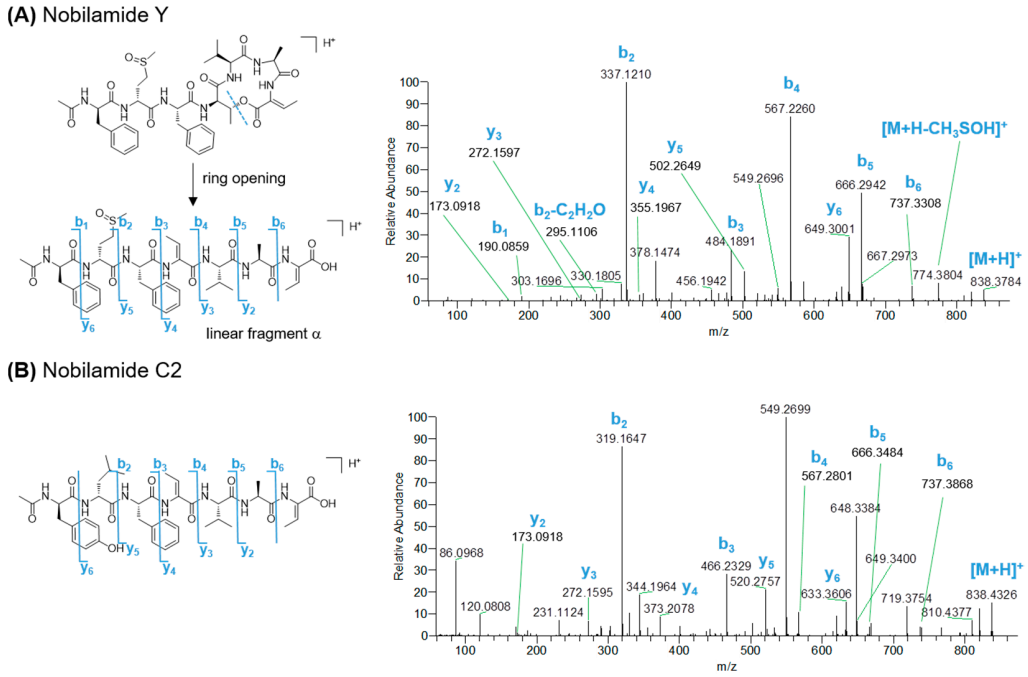

Figure 5. HRMS^2 spectra of the [M + H]$^+$ pseudomolecular ions of representative cyclic (**A**) and linear (**B**) nobilamides from *Bacillus* sp. BCP32.

Phe^1 is replaced by either Leu, Met, methionine sulfoxide (MetO), or Tyr in a few congeners. When MetO is incorporated, the product ion spectra of nobilamides display fragment ions arising from the neutral loss of methanesulfenic acid (CH_3SOH, 63.9983 Da), which is indicative of the sulfoxide group inside chain of MetO. Leu^2 is conserved across all depsiheptapeptides and linear heptapeptides except nobilamide X and Y, which feature MetO at position 2. Met, MetO, and Leu are also found in place of Phe^3 in some congeners; notably, nobilamide F2 bears an unprecedented putative kynurenine (Kyn) residue at position 3, as shown by the neutral loss of 190.0742 Da ($C_{10}H_{10}N_2O_2$) from the y_5 and b_3 ions (Figure S48). In general, by analogy with the nobilamide structures described so far, we tentatively discriminated between the isobaric Ile and Leu residues, thus assigning Leu at positions 1, 2, and 3 where present. Interestingly, this assignment was corroborated by the A domain substrate selectivity predicted in silico (see Section 2.7). Nobilamide depsiheptapeptides and linear heptapeptides from *Bacillus* sp. BCP32 share Thr^4, with only two congeners, i.e., nobilamide L1 and L2, including Ser^4. The most frequent amino acid at position 5 is Val, even if either Ile/Leu, Phe, Ala, *homo*-Ala, or Thr are incorporated in minor isoforms. We tentatively distinguished between the isomeric *homo*-Ala and *N*-Me-Ala in nobilamide B2 as *homo*-Ala was already reported in the structural analogue nobilamide M [47]. Ala^6 is replaced by either Gly, Ser, or Thr, while the last amino acid is most cases represented by (*Z*)-2,3-dehydrobutyrine, which can be substituted by Thr. Notably, the presence of diaminobutyric acid (Dab) in nobilamide B1, phenethylamine (Pea) in nobilamide Q2, and tyramine (Tym) in nobilamide J2 was observed at position 7, thus unveiling unique structural variations in the nobilamide family from *Bacillus* sp. BCP32.

Most nobilamide depsiheptapeptides and linear heptapeptides undergo N-terminal acetylation. Nevertheless, isoforms having propanoyl, isobutanoyl, and C_5H_9O acyl groups have been identified together with deacylated derivatives.

The stereochemistry of the seven amino acids was assigned through bioinformatic prediction and by analogy with the stereochemistry of nobilamides determined by Marfey's method and NMR spectroscopy [35,47]. As the nobilamide synthetase includes three epimerization domains within modules 1, 2, and 4 (Figure 6), respectively, the presence of D-

Phe[1], D-Leu [2] and D-*allo*-Thr [4] was inferred, while the remaining amino acids were assumed to possess the L configuration. The genomics-driven absolute configuration assignment turned out to be in agreement with the reported stereochemistry for nobilamides.

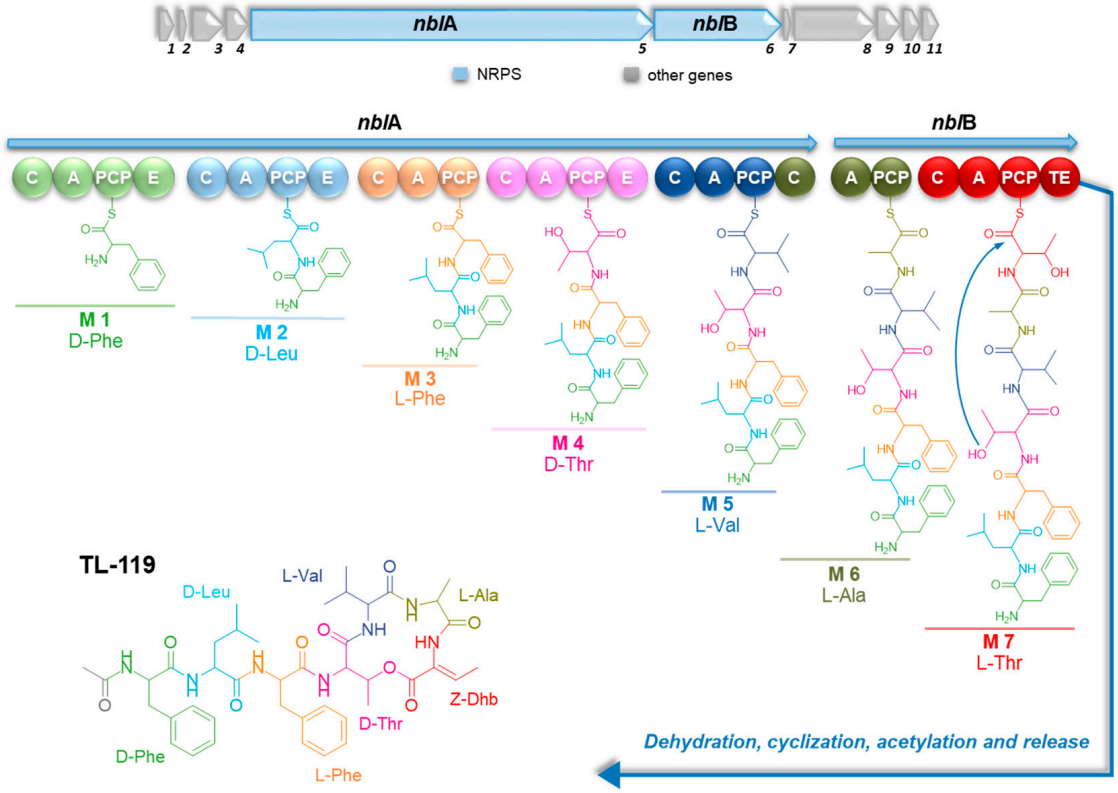

Figure 6. Putative biosynthesis of TL-119. Genes flanking the *nbl* operon are annotated in Table S5. Abbreviations: C, condensation domain; A, adenylation domain; PCP, peptidyl-carrier protein; E, epimerase; TE, thioesterase.

The F-90% MeOH was separated by reversed phase HPLC chromatography, thus yielding the pure cyclic depsiheptapeptides TL-119 and nobilamide I, and the novel congeners T1 and S1, that were assessed for antimicrobial activity (see Section 2.6).

2.5. Structural Characterization of Cyclic and Linear Hexa-, Octa-, and Nonapeptides by Mass Spectrometry

Manual inspection of the nobilamide cluster within the molecular network led to the identification of cyclic N-acyldepsihexapeptides and linear hexapeptides (Tables 4 and 5). These congeners bear the same structural features as cyclic depsiheptapeptides and linear heptapeptides, except for nobilamide A3 having an unusual $C_6H_9O_2$ acyl group, tentatively identified as a 4-methyl-2-oxovaleryl moiety, which may either be recruited by the first NRPS module of the Nbl synthetase [49] or derive from oxidative deamination of a leucine starter unit. Cyclic nobilamides R2-U2, V2, and W2 and linear nobilamides C3 and E3 are truncated isoforms at the N- or C-terminus of the cognate heptapeptide analogues, while nobilamides X2-B3 and D3 are closely related to the already known nobilamide D, where the second amino acid, i.e., D-Leu, is missing. These findings suggest that modules 1, 2, and 7 of the Nbl synthetase might be skipped for the generation of the truncated congeners, likely as a result of an aberrant event leading to the production of minor metabolites [50]. While module skipping processes occurred in several PKSs and hybrid PKS/NRPS systems, this event has been described only once for multimodular NRPS so far, and that is the case of myxochromide S biosynthesis [51].

Differently from the other nobilamide-producing strains, *Bacillus* sp. BCP32 showed the biosynthetic ability to assemble cyclic octa- and nonadepsipeptides and linear octapeptides (Tables 6–8). Nobilamides F3 and G3 are cyclic octadepsipeptides which differ from TL-119 as having an additional amino acid at the C-terminus, i.e., L-dehydro-Asn and L-Thr, respectively, involved in the formation of the lactone ring with the side-chain OH group of D-*allo*-Thr^4 (Figures S73 and S74). Linear octapeptides H3-O3 have the hexapeptide motif Phe^1-D-Leu^2-L-Phe^3-D-*allo*-Thr^4/Dhb^4-L-Val^5-L-Ala^6, while structural diversification results in amino acid substitutions in positions 7 and 8 (Figures S75–S82). Indeed, either L-Thr, L-Thr-O-methyl ether, or (*Z*)-2,3-dehydrobutyrine is incorporated at position 7, whereas Pea, Tym, Leu/Ile, Phe, or Ala may occupy position 8. Considering that Nbl synthetase includes only seven modules, it can be argued that cyclic octadepsipeptides may derive from the iterative use of module 7, which is expected to allow for the accommodation of L-dehydro-Asn and L-Thr—structurally similar amino acids—and catalyze cyclization for the assemblage of nobilamides F3 and G3. On the other hand, linear octapeptides H3-O3 apparently derive from linear/cyclic heptapeptides, which could undergo spontaneous nucleophilic acyl substitution at the C-terminus with aromatic amines (Pea, Tym) or amino acids. It has been demonstrated that aromatic amine accumulation, due to amino acid decarboxylation, may provide building blocks for spontaneous condensation reactions, leading to the biosynthesis of imidazolium alkaloids, i.e., discolins, from *Tenacibaculum discolor* sv11 [52]. However, it cannot be excluded that a TE domain, as reported for bacillothiazols [53], or even a C-type domain present elsewhere in the chromosome, as speculated for crochelins [54], may be involved in the addition of the additional C-terminus moieties beyond the prediction of the heptamodular assembly line [55].

Table 8. Cyclic depsinonapeptide from *Bacillus* sp. BCP32. [a] The D-*allo*-Thr^6 side-chain OH group forms an ester bond with the C-terminal residue. Abbreviations: Nob, nobilamide; Ac, acetyl; D-*a*-Thr, D-*allo*-threonine.

Nob	[M + H]$^+$	*m*/*z*	R_t (min)	R_1	aa-1	aa-2	aa-3	aa-4	aa-5	aa-6 [a]	aa-7	aa-8	aa-9
P3	$C_{51}H_{76}N_9O_{13}$	1022.5545	18.8	Ac	D-Phe	D-Leu	L-Phe	D-*a*-Thr	L-Val	D-*a*-Thr	L-Val	L-Ala	L-Thr

The peptide backbone of nobilamide P3 was determined as Phe^1-D-Leu^2-L-Phe^3-D-*allo*-Thr^4-L-Val^5-D-*allo*-Thr^6-L-Val^7-L-Ala^8-L-Thr^9, where the D-*allo*-Thr^6 side-chain OH group was predicted to form an ester bond with the C-terminal L-Thr^9 (Table 8, Figure S83). Biosynthetically, nobilamide P3 may result from an aberrant process where modules 4 and 5 are used twice to generate this nonapeptide lactone, which is unusual among its congeners.

2.6. Surfactant and Antibacterial Activity of Nobilamides and Surfactins

Aiming to correlate surfactant and antibacterial activities to specific metabolites (Figure S3), F-90% MeOH was subjected to HPLC to obtain pure nobilamides T1, I, TL-119, and S1, as well as surfactin C and a mixture of two isomers of surfactin B, featuring identical MS^2 spectra, which could not be resolved (major isomer 56%, minor isomer 44%) (Figure S4).

Surfactins demonstrated high biosurfactant activity in the oil spreading test (Figure S3) and antimicrobial activity against the human pathogens *S. aureus* 6538 and 6538p (MIC values ranging from 15.6 to 64.5 μg/mL) (Table S2). No activity was observed against antibiotic-resistant *S. aureus* strains, *S. epidermidis*, *S. xylosus*, and *L. monocytogenes*.

Due to the lack of antibacterial activity against the Gram-negative bacterium *E. coli* ATCC 10536, nobilamides T1, I, TL-119, and S1 were evaluated against a panel of Gram-positive pathogens. TL-119 was the most potent antibacterial agent, with MIC values

ranging from 0.24 µg/mL to 7.8 µg/mL towards all tested pathogens, while no nobilamides showed activity against VRSA (Table 9). This could suggest that nobilamides may have a mechanism of action similar to that of vancomycin, which targets bacterial membranes by inhibiting cell wall synthesis [56,57].

Table 9. Antibacterial activity of nobilamides from *Bacillus* sp. BCP32 towards a panel of Gram-positive pathogens. [a] Vancomycin, [b] erythromycin, and [c] ampicillin were used as positive controls. MIC values are expressed in µg/mL.

Strain	Nobilamide T1	Nobilamide I	Tl-119	Nobilamide S1	Positive Control
S. aureus 6538p	-	-	0.24	15.6	1 [a]
S. aureus 6538	-	-	0.24	7.8	0.5 [a]
S. aureus methicillin-resistant	-	-	3.9	-	0.5 [a]
S. aureus macrolide-resistant	-	-	1.9	-	0.5 [a]
S. aureus quinolone-resistant	-	-	0.9	-	0.5 [a]
S. aureus vancomycin-resistant	-	-	-	-	1 [b]
S. epidermidis RP206	-	-	7.8	-	0.5 [a]
S. xilosus MB5209	-	-	7.8	31.5	0.5 [a]
L. monocytogenes 677	-	-	0.24	3.9	1 [c]

Interestingly, even if less active as compared to TL-119, the novel nobilamide S1 maintained potent growth inhibition towards *S. aureus* 6538, *S. aureus* 6538p, and *L. monocytogenes* 677, and mild effects against *S. xilosus* MB5209 (Table 9). To the best of our knowledge, this is the first time that nobilamides demonstrated antibiotic activity towards *Listeria* and antibiotic-resistant *Staphylococcus* strains.

These findings unveiled the structural features that are essential for maintaining growth inhibitory effects against the panel of human pathogens reported in Table 9. The absence of the N-acetyl group on Phe^1 led to the loss of bioactivity in nobilamide T1, although having the same peptide backbone as the N-acetyl encapped TL-119. In addition, Dhb^7 is crucial to keep the antibiotic activity of TL-119, as the molecule became inactive when replaced by Thr as in nobilamide I. The $Val^5 \rightarrow Leu/Ile^5$ substitution observed in nobilamide S1 markedly weakened the growth inhibitory properties of TL-119. Finally, previous results revealed the lactone ring—and the C-terminal Dhb—as a key structural motif for the antimicrobial effects of nobilamides against *S. aureus* and *L. sphaericus* [47].

Nobilamides did not show any activity in the oil spreading test, thereby indicating that only surfactins are responsible for the surfactant effects of F-90% MeOH (Figure S3).

2.7. Genome-Based Bacterial Identification and Elucidation of Nobilamide Biosynthetic Gene Cluster

Bacillus sp. BCP32 was subjected to whole genome sequencing for the correct taxonomical assignment of the species and to search for BGCs encoding the discovered compounds. DNA sequencing was performed using both Illumina short-read sequencing and Oxford Nanopore technology's long-read sequencing, thus yielding the complete closed genome sequence. BCP32 genome has a total length of 4.197.037 bp with a G + C content of 43.76%. The analysis of its 16S rRNA gene through EzBioCloud [58,59] revealed a high similarity with *Bacillus halotolerans* ATCC 25096 (99.93%), *Bacillus mojavensis* RO-H-1 (99.86%), and *Bacillus cabrialesii* TE3 (99.80%). The BCP32-assembled genome was compared with the genomes of the above-mentioned strains using the OrthoANI Genomic Similarity tool. *Bacillus* sp. BCP32 shared the highest ANI value with *B. halotolerans* ATCC 25096 (98%), thus allowing for species assignment. The presence of *B. halotolerans* has already been reported from deep-sea and salty environments, demonstrating its capability to adapt to extreme conditions [42,60,61].

Although the first member of the nobilamide family, i.e., TL-119, was discovered in 1975 [33], there is no evidence about nobilamide biosynthesis to date. Aiming to detect the biosynthetic pathway for nobilamides, the *Bacillus* sp. BCP32 genome was mined by antiSMASH [62] for NRPS and RiPP BGCs, which are known to assemble peptide secondary metabolites. AntiSMASH enabled the detection of six NRPS and RiPP pathways, including the surfactin, bacillaene, bacillabactin, fengycin, subtilosin A, and a putative novel multimodular NRPS BGCs. Nobilamide biosynthesis was inferred to be directed by this orphan multimodular NRPS, designated as Nbl, based on the collinearity between the adenylation (A) domain specificity within each NRPS module and the chemical structure of TL-119 (see Table S3). The putative *nbl* operon is 27,723 bp long and is made up of seven NRPS modules. An in silico prediction of the A domain substrate selectivity nicely correlates with the consensus sequence D-Phe^1-D-Leu^2-L-Phe^3-D-*allo*-Thr^4-L-Val^5-L-Ala^6-(*Z*)-Dhb^7, inferred by the MS-based structural characterization of cyclic depsiheptapeptides and linear heptapeptides (Section 2.4), except for Dhb^7 (Figure 6, Table S3). Indeed, antiSMASH analysis predicted Nbl_A7 to recruit Thr, and this is likely true considering that Dhb^7 may derive from Thr dehydration. The incorporation of dehydroamino acids, such as Dhb and Dha (α,β-dehydroalanine), in non-ribosomal peptides has been reported to involve a threonine/serine dehydration step, which can be catalyzed either by the so-called "modified AA" condensation domains (C_{modAA}), such as AlbB_C_{modAA} in albopeptide biosynthesis, or by a distinct class of $^{D}C_{L}$ domains, such as NocB_C5 in nocardicin biosynthesis [63]. The *nbl* gene cluster apparently lacks a C domain in the last module, which can presumably participate in Thr dehydration, as Nbl_C7 did not cluster with any of these unique C domains in a phylogenetic analysis performed with NaPDoS [64]. Therefore, it remains unclear whether Nbl_C7 or an auxiliary tailoring enzyme is responsible for the dehydration of Thr^7 and how this mechanism is regulated to generate Dhb^7 or Thr^7–containing nobilamide isoforms. Three typical epimerization domains are present in modules 1, 2, and 4, thereby suggesting the D configuration for aa^1, aa^2, and aa^4 of cyclic depsiheptapeptides and linear heptapeptides of the nobilamide family, which is consistent with the reported stereochemistry for nobilamides. The last module terminates with a canonical thioesterase (TE) domain, which is expected to catalyze the peptide release through hydrolysis or cyclization to give linear or cyclic nobilamides, respectively. Most nobilamide variants bear an acyl group at the N-terminus, which is in most cases represented by an acetyl unit. *N*-acetylated cyclic peptides are extremely rare in nature. Beyond nobilamides, chaiyaphumines from *Xenorhabdus* sp. PB61.4, heptarhizin from the endosymbiotic bacterium *Burkholderia rhizoxinica*, and griselimycins from *Streptomyces muensis* DSM 40835 are among the few *N*-acetyl encapped peptides reported to date [65–67]. Following a typical lipoinitiation strategy [68], starter C domains (Cs) catalyze the N-acetylation of the nonribosomal peptides griselimycins and heptarhizin. However, Nbl synthetase lacks a canonical Cs domain, although featuring a C domain in the first module, which obviously does not share significant similarity with Cs domains deposited in the NaPDoS database. Therefore, the acetylation mechanism remains elusive, raising the question of whether Nbl_C1 may acylate nobilamides at the N-terminus. In addition, acyltransferases or acyl-CoA ligases, presumably located in a different locus of the bacterial genome, could participate in nobilamide acetylation.

Interestingly, the detection of nobilamide variants containing more/less than seven amino acids clearly indicates that the Nbl synthetase may deviate from the canonical "collinearity" rule. The generation of these "odd", minor isoforms can be traced back to aberrant biochemical processes, such as module skipping or the iterative use of specific modules, rather than programmed biosynthetic events. In addition, following amine/amino acids accumulation, spontaneous nucleophile-mediated ring opening reactions could trigger the formation of unexpected linear octapeptide congeners from cyclic heptadepsipeptides.

These processes, together with the relaxed substrate selectivity of the Nbl adenylation domains, have contributed to expand the chemical diversity of the nobilamide family.

3. Materials and Methods

3.1. Primary Screening

The SZN bacterial library was subjected to a primary screening in order to select promising strains for the production of the molecules of interest. Micro-cultivation was carried out in 96 multiwell plates. After 2 days of incubation in the most suitable medium at 20 °C under shaking conditions, 20 µL of microcultures were transferred into a new 96-deepwell (catalog number: 278743, Thermo Fisher Scientific™, Waltham, MA, USA) with different growth media. Secondary metabolite production was evaluated at a range of 3–10 days of cultivation, at temperatures between 10 and 37 °C. Afterwards, the cultures were centrifuged to separate the cells from the supernatant, which was then transferred into a new deep well plate. Particularly, 10 µL of the supernatant were used for biosurfactant assays (CTAB agar assay and oil displacement test) and 100 µL was used for the agar well diffusion assay to assess antibacterial activity.

3.2. Strain Identification

The strain *Bacillus* sp. BCP32 was isolated from a 450 m deep-sea sediment sample collected from the Dohrn Canyon, 19 km off the coast of the Gulf of Naples (Italy). The strain was identified as belonging to the genus *Bacillus* via 16S rRNA gene amplification and subsequent phylogenetic analysis. PCR was carried out in a total volume of 40 µL, containing 25 µL of PCR Master Mix 2× ExtraWhiteTaq (a ready-to-use solution containing TaqPol, buffer, $MgCl_2$ and dNTPs), and 0.2 µM of both primers, 27F (Forward, seq: 5′-AGAGTTTGATCCTGGCTCAG-3′) and 1492R (Reverse, seq 5′-GGTTACCTTGTTACGACTT-3′) [69]. PCR was carried out under the following conditions: initial denaturation at 95 °C for 5 min, followed by 33 cycles of 95 °C for 30 s, 58 °C for 30 s, and 72 °C for 90 s, with a final extension at 72 °C for 7 min.

Afterwards PCR products were evaluated on 1% agarose gel, then purified with the GeneAll kit and sequenced by Eurofins Genomics. Finally, the phylogenetical affiliation was assigned using the EzBioCloud (http://ezbiocloud.net, accessed on 18 June 2024).

3.3. Bacterial Cultivation, Chemical Extraction, and Compounds Isolation

After the selection of *Bacillus* sp. BCP32 as one of the most active strains in the SZN library, a single colony of the bacterial isolate was used to inoculate 3 mL of liquid TYP medium (16 g/L bacto-tryptone, 16 g/L yeast extract, 10 g/L NaCl) in sterile bacteriological tubes. After 48 h of incubation at 20 °C at 200 rpm, the preinoculum was used to inoculate 4 × 250 mL flasks, each containing 50 mL of TYP medium, at a concentration of 0.01 OD_{600}/mL. Bacterial cultures were incubated at 28 °C under shaking (150 rpm) for 48 h. Then, cultures were centrifuged at 7500 rpm at 4 °C for 30 min to collect supernatants, which were extracted with two volumes of EtOAc. Successively, organic phases were combined and evaporated with a rotary evaporator (Buchi R-100, Büchi Labortechnik AG, Postfach, Switzerland) to afford the crude extract. Finally, the obtained extract was dissolved in DMSO at 50 mg/mL and stored at 4 °C to be tested for bioactivities.

For the large-scale fermentation of *Bacillus* sp. BCP32 and subsequent compounds isolation, 4× 1 L flasks, each containing 250 mL of TYP medium, were inoculated at an initial concentration of 0.01 OD_{600}/mL and incubated at 28 °C under shaking (150 rpm). After two days, the aforementioned extraction protocol was performed to obtain the crude extract from the exhausted culture broth. The EtOAc extract (430 mg) was fractionated into five fractions by solid-phase fractionation (SPE), using a reverse-phase Chromabond C-18

column Cartridge (Macherey-Nagel GmbH & Co. KG, Duren, Germany). Briefly, the extract was resuspended in the minimum volume of MeOH and uploaded onto the pre-activated SPE column. The elution was performed with two column volumes of different mixtures of MeOH and H_2O, as follows: (1) 100% H_2O, (2) 50% MeOH/H_2O (v/v), (3) 90% MeOH/H_2O (v/v), (4) 100% MeOH, and (5) MeOH + 0.1%TFA. Aliquots of the obtained fractions were dissolved in DMSO at 50 and 25 mg/mL to perform antibiotic and biosurfactant assays. The 90% MeOH fraction (F-90% MeOH) (238.2 mg) was subjected to reverse-phase HPLC separation on a semi-preparative Jupiter Proteo column (4 µm, 250 × 10 mm), thus affording nobilamide T1 (R_t = 6.8 min, 1.5 mg), nobilamide I (R_t = 8.6 min, 5.2 mg), TL-119 (R_t = 11.1 min, 6.4 mg), nobilamide S1 (R_t = 12.7 min, 1.9 mg), surfactin A (R_t = 21.9 min, 4.4 mg), surfactin B (mixture of two isomers, R_t = 22.7 min, 7.6 mg), and surfactin C (R_t = 23.6 min, 26 mg). The column was eluted at room temperature at a flow rate of 5 mL/min with H_2O and CH_3CN (both eluents supplemented with 0.1% TFA), following the gradient elution programme: 0–60% CH_3CN 0–1 min, 60−75% CH_3CN 1–14 min, 75−85% CH_3CN 14–15 min, 85–100% CH_3CN 15–35 min. Detection was achieved at a 210 nm wavelength.

3.4. LC-HRMS^2 Analysis of the 90% MeOH Fraction

The F-90% MeOH fraction obtained from the *Bacillus* sp. BCP32 crude extract was dissolved in MeOH at 1 mg/mL for LC-HRMS^2 analysis, as previously described [70]. Chemical profiling was conducted using a Thermo Scientific Q Exactive Focus Orbitrap mass spectrometer coupled to a Thermo Ultimate 3000 HPLC system equipped with a Hypersil C18 column (100 × 4.6 mm, 3 µm). The column was eluted at room temperature at a flow rate of 400 µL/min with H_2O (containing 0.1% HCOOH) and CH_3CN, following the gradient elution programme: 25% CH_3CN for 3 min, 25−80% CH_3CN over 60 min, and 95% CH_3CN for 7 min. Mass spectra were recorded in positive ion mode with a mass accuracy of ≤3 ppm. The MS parameters were as follows: spray voltage of 4.8 kV, capillary temperature of 285 °C, sheath gas flow rate of 32 units N_2 (~150 mL/min), and auxiliary gas flow rate of 15 units N_2. MS^2 data were collected in data-dependent acquisition mode to fragment the three most intense ions from a full-scan mass spectrum, with an m/z range of 50 to 2000 Daltons. HRMS^2 scans were performed by HCD fragmentation, using an isolation width of 2.0 m/z, a normalized collision energy of 15 units, and an automated injection time.

3.5. Feature-Based Molecular Networking

Raw files from LC-HRMS^2 analysis of the F-90% MeOH fraction were processed by MZmine 2.53, using parameters reported in Table S4 to obtain a .mgf file. This file was employed as input on the GNPS2 Analysis Hub (https://gnps2.org, accessed on 2 October 2024) [71] to build a molecular network with the feature-based molecular networking (FBMN) workflow [72]. For FBMN analysis, the precursor ion mass tolerance was set to 0.02 Da, and the MS^2 fragment ion tolerance was set to 0.05 Da. Subsequently, a molecular network was constructed, setting the maximum number of nodes in one cluster to 100, with edges filtered to have a cosine score above 0.7 with a minimum of four matching peaks. Analogues were also searched, not exceeding the difference of 300 Da between the query and the hit; the analogues had to follow the same clustering rules as mentioned above. Finally, the network was visualized using the Cytoscape software v. 3.8.2 and can be publicly accessed at https://gnps2.org/status?task=1b1c1180d47d47debeeea7f688d989fb, accessed on 2 October 2024.

3.6. Biosurfactant and Antimicrobial Assays

Biosurfactant and antimicrobial assays were performed to assess the bioactivity of crude extracts, SPE fractions, and purified compounds.

3.6.1. Biosurfactants Assays

Biosurfactant-producing bacteria were screened using the cetyltrimethylammonium bromide (CTAB) agar assay [73] and the oil displacement test [74].

- CTAB Agar Assay

The CTAB agar plates method is a semi-quantitative test for the detection of anionic surfactants which was devised by Wagner and Siegmund [73]. The test is positive if the extracts contain anionic surfactants due to the formation of an insoluble ion pair between the anionic biosurfactant, CTAB, and methylene blue. Therefore, positivity is revealed by the dark blue halos around the extracts. For this assay, 1 µL of the extracts at 50 mg/mL, dissolved in DMSO were spotted on the blue agar plates. As a negative control, 4 µL of pure DMSO were used, while 4 µL of 0.1% and 0.01% sodium dodecyl sulphate (SDS) were used as positive controls. After 2 days at 4 °C, the extracts containing biosurfactants were selected by the presence of a dark blue halo around.

- Oil Displacement Test

The oil spreading assay, also called the oil displacement test [74], was performed in a Petri dish of polystyrene containing 40 µL of crude oil added to the surface of 40 mL of distilled water to form a thin oil layer. Then, 10 µL of culture supernatant or 1 µL of extracts at 50 mg/mL were gently placed on the centre of the oil layer. The diameter of the clear zone on the oil surface is related to surfactant activity, due to the presence of the biosurfactant that displaces the oil.

3.6.2. Antimicrobial Assays

- Agar Well-Diffusion Method

To assess the antibacterial activity of the 300 bacteria screened, the agar well-diffusion method (ADM) was performed against *Escherichia coli* ATCC® 10536™ and *Staphyloccus aureus* ATCC® 6538™. This method involves inoculating an agar plate with a standardized microbial inoculum and placing 100 µL of culture supernatants into the agar through wells previously obtained, as shown in Figure 1. The sample diffuses into the medium for 24 h at 37 °C, and if the sample has activity, a zone of inhibition forms around the applied area, which is measured to assess the level of effectiveness [75].

- Liquid Inhibition Assay

To evaluate the antimicrobial potential of all samples, the MICs for *E. coli* ATCC® 10536™, *S. aureus* ATCC® 6538™, *S. aureus* ATCC® 6538p™, methicillin-resistant *S. aureus* (MRSA), macrolide-resistant *S. aureus* (MRSA), quinolone-resistant *S. aureus* (QRSA), vancomycin-resistant *S. aureus* (VRSA) [76], *S. epidermidis* RP206 [7], *S. xylosus* MB 5209 [77] were determined by the liquid inhibition assay [78]. Briefly, the bacterial strains were inoculated in 3 mL of liquid Mueller–Hinton broth (MHB) (HiMedia, Einhausen, Germany) in sterile bacteriological tubes and incubated in agitation at 37 °C until they reached the turbidity of 0.5 McFarland. Different from the remaining pathogens, *L. monocytogenes* MB 677 [79] was diluted in the Trypticasein soy broth (TSB) medium with an additional 0.6% yeast extract. Finally, serial dilutions of the inoculum were performed to obtain a final bacterial concentration of about 5×10^5 CFU/mL. Then, 4 µL of each sample was added into a 96-well microtiter plate containing 200 µL of MH medium. After being serially diluted using MH medium, 100 µL of bacterial suspension was inoculated into the broth

(~5 × 10^4 CFU/well) and incubated statically for 18 h at 37 °C. DMSO was used as a control to determine the effect of solvent on cell growth. Vancomycin, erythromycin, and ampicillin were used as positive controls. The MIC was identified as the lowest concentration that completely inhibited the growth of the pathogens, which was measured as the absorbance at 600 nm by using a ELX800 Absorbance Microplate Reader (Biotek, Winoosky, VT, USA).

3.7. Whole-Genome Sequencing and Bioinformatics

A total of 1 µg of genomic DNA was used for whole genome sequencing of *Bacillus* sp. BCP32, which was performed by Eurofins Genomics (Ebersberg, Germany) using the Illumina NovaSeq 6000 platform. All sequenced paired ends reads were clipped and trimmed with Trimmomatic tool [80] to remove adaptor and low-quality sequences, and a quality check was obtained with FastQC [81]. The bacterial genome was assembled with the MEGAhit algorithm [82], employing the genome of *B. halotolerans* ZB201702 (NZ_CP029364.1) as a reference to direct the arrangement and alignment of contigs. In addition, the whole genome was re-sequenced using Oxford Nanopore Technology (ONT) [83] to obtain longer reads, sending 30 µL of genomic DNA at 20 ng/mL to Eurofins Genomics. Then, to obtain a closed genome, a hybrid assembly was performed by the bioinformatic tool Unicycler [84] on the Galaxy Europe 0.5.0 server (https://usegalaxy.eu/, accessed on 12 June 2024), by inputting the raw data of both sequencing processes [85]. The assembled genome identification was carried out using the ANI Calculator by EzBioCloud [58] and the digital DNA–DNA hybridization (dDDH) analysis by Type (strain) Genome Server (https://tygs.dsmz.de, accessed on 14 June 2024). Subsequently, the assembly was analyzed using the genome mining tool antiSMASH 7.0, which led to the identification of biosynthetic gene clusters (BGCs). The nobilamide gene cluster and the whole bacterial genome of *Bacillus* sp. BCP32 were deposited in GenBank under accession numbers PQ787232 and CP176792, respectively.

4. Conclusions

In this study, the exploration of marine microbial biodiversity using a rapid and effective screening allowed for the identification of a deep-sea *Bacillus* of biotechnological interest. The strain was able to produce both antimicrobial and biosurfactant metabolites in the same growth conditions. Feature-based molecular networking analysis of the bacterial exometabolome shed light on the presence of two molecular families, namely surfactins and nobilamides, thereby explaining the observed bioactivities. The manual inspection of MS^2 spectra of the nobilamide cluster enabled the structural characterization of 84 nobilamide congeners, 71 being novel molecules, thus expanding the outstanding chemical diversity of these non-ribosomal peptides. The well-known TL-119 and the novel congener nobilamide S1 were isolated as pure compounds and shown to be promising antibiotics against a range of Gram-positive bacteria, including several *S. aureus* strains, *S. xylosus*, and *L. monocytogenes*. A significant finding of this study was the potent activity of TL-119 and nobilamide S1 against the foodborne pathogen *Listeria*, which has been demonstrated for the first time, suggesting that nobilamides could be an alternative to β-lactams in the treatment of listeriosis. In addition, the novelty of this work lies in elucidating the previously unknown BGC of nobilamides. Future efforts will foresee the scale-up of *Bacillus* sp. BCP32 culture in order to purify most of the novel nobilamides identified so far and assess them for antibiotic activity.

Supplementary Materials: The following supporting information can be downloaded at: https://www.mdpi.com/article/10.3390/md23010041/s1, Table S1: Antibacterial activity of SPE fractions from *Bacillus* sp. BCP32 crude extract towards a panel of Gram-positive pathogens; Table S2: Antibacterial activity of surfactins B (mixture of two isomers) and C; Table S3: Binding pocket signatures of adenylation domains from the Nbl synthetase; Table S4: MZmine2 parameters for MS raw data processing; Table S5: Putative genes flanking the *nbl* gene cluster; Figure S1: Surfactant activity evaluation of SPE fractions from *Bacillus* sp. BCP32 by oil spreading test; Figure S2: Ring opening of cyclic nobilamides during mass fragmentation; Figure S3: Surfactant activity evaluation of nobilamides T1, I, TL-119, and S1 and surfactins A, B, and C; Figure S4: LC-HRMS^2 chromatograms (upper panel) and MS^2 spectra (lower panel) of surfactin B isomers (a) and surfactin C (b); Figures S5–S83: HRMS^2 spectra of nobilamides.

Author Contributions: Conceptualization, F.P.E. and G.D.S.; methodology, V.C., F.P.E. and G.D.S.; validation, V.C., F.P.E. and G.D.S.; formal analysis, F.P.E., P.T., D.C. and G.D.S.; investigation, F.P.E., G.D.S., V.C., C.R., G.A.V. and C.B.; resources, D.d.P.; data curation, V.C., F.P.E., S.S. and G.D.S.; writing—original draft preparation, V.C., F.P.E. and G.D.S.; writing—review and editing, F.P.E., P.T., D.C. and G.D.S.; visualization, P.T. and D.C.; supervision, F.P.E., D.d.P. and G.D.S.; project administration, D.d.P.; funding acquisition, D.d.P. All authors have read and agreed to the published version of the manuscript.

Funding: This research was funded by H2020-FNR-11-2020: SECRETED—Grant agreement: 101000794.

Institutional Review Board Statement: Not applicable.

Data Availability Statement: The molecular networks and mass spectrometry data can be publicly accessed at https://gnps2.org/status?task=1b1c1180d47d47debeeea7f688d989fb, accessed on 2 October 2024. The nobilamide gene cluster and the whole genome of *Bacillus* sp. BCP32 were deposited in GenBank under accession numbers PQ787232 and CP176792, respectively.

Conflicts of Interest: The authors declare no conflict of interest.

References

1. Zhao, X.-Q. Genome-Based Studies of Marine Microorganisms to Maximize the Diversity of Natural Products Discovery for Medical Treatments. *Evid. Based Complement. Altern. Med.* **2011**, *2011*, 384572. [CrossRef] [PubMed]
2. GBD 2021 Antimicrobial Resistance Collaborators. Global Burden of Bacterial Antimicrobial Resistance 1990–2021: A Systematic Analysis with Forecasts to 2050. *Lancet* **2024**, *404*, 1199–1226. [CrossRef] [PubMed]
3. Antimicrobial Resistance: A Silent Pandemic. *Nat. Commun.* **2024**, *15*, 6198. [CrossRef] [PubMed]
4. Xie, C.-L.; Xia, J.-M.; Wang, J.-S.; Lin, D.-H.; Yang, X.-W. Metabolomic Investigations on Nesterenkonia Flava Revealed Significant Differences between Marine and Terrestrial Actinomycetes. *Mar. Drugs* **2018**, *16*, 356. [CrossRef]
5. Ajar Nath, Y. Microbial Biotechnology for Bio-Prospecting of Microbial Bioactive Compounds and Secondary Metabolites. *J. Appl. Biol. Biotechnol.* **2021**, *9*, 1–6. [CrossRef]
6. Magiorakos, A.-P.; Srinivasan, A.; Carey, R.B.; Carmeli, Y.; Falagas, M.E.; Giske, C.G.; Harbarth, S.; Hindler, J.F.; Kahlmeter, G.; Olsson-Liljequist, B.; et al. Multidrug-Resistant, Extensively Drug-Resistant and Pandrug-Resistant Bacteria: An International Expert Proposal for Interim Standard Definitions for Acquired Resistance. *Clin. Microbiol. Infect.* **2012**, *18*, 268–281. [CrossRef] [PubMed]
7. Kannappan, A.; Sivaranjani, M.; Srinivasan, R.; Rathna, J.; Pandian, S.K.; Ravi, A.V. Inhibitory Efficacy of Geraniol on Biofilm Formation and Development of Adaptive Resistance in Staphylococcus Epidermidis RP62A. *J. Med. Microbiol.* **2017**, *66*, 1506–1515. [CrossRef] [PubMed]
8. Chianese, G.; Esposito, F.P.; Parrot, D.; Ingham, C.; De Pascale, D.; Tasdemir, D. Linear Aminolipids with Moderate Antimicrobial Activity from the Antarctic Gram-Negative Bacterium *Aequorivita* sp. *Mar. Drugs* **2018**, *16*, 187. [CrossRef]
9. Palma Esposito, F.; Ingham, C.J.; Hurtado-Ortiz, R.; Bizet, C.; Tasdemir, D.; de Pascale, D. Isolation by Miniaturized Culture Chip of an Antarctic Bacterium *Aequorivita* sp. with Antimicrobial and Anthelmintic Activity. *Biotechnol. Rep.* **2018**, *20*, e00281. [CrossRef]
10. De Oliveira, D.M.P.; Forde, B.M.; Kidd, T.J.; Harris, P.N.A.; Schembri, M.A.; Beatson, S.A.; Paterson, D.L.; Walker, M.J. Antimicrobial Resistance in ESKAPE Pathogens. *Clin. Microbiol. Rev.* **2020**, *33*, e00181-19. [CrossRef]
11. Newman, D.J.; Cragg, G.M. Natural Products as Sources of New Drugs over the 30 Years from 1981 to 2010. *J. Nat. Prod.* **2012**, *75*, 311–335. [CrossRef] [PubMed]

12. Bologa, C.G.; Ursu, O.; Oprea, T.I.; Melançon, C.E.; Tegos, G.P. Emerging Trends in the Discovery of Natural Product Antibacterials. *Curr. Opin. Pharmacol.* **2013**, *13*, 678–687. [CrossRef] [PubMed]
13. Kaur, P.; Li, Y.; Cai, J.; Song, L. Selective Membrane Disruption Mechanism of an Antibacterial γ-AApeptide Defined by EPR Spectroscopy. *Biophys. J.* **2016**, *110*, 1789–1799. [CrossRef]
14. Bechinger, B.; Gorr, S.-U. Antimicrobial Peptides: Mechanisms of Action and Resistance. *J. Dent. Res.* **2017**, *96*, 254–260. [CrossRef]
15. Giugliano, R.; Della Sala, G.; Buonocore, C.; Zannella, C.; Tedesco, P.; Palma Esposito, F.; Ragozzino, C.; Chianese, A.; Morone, M.V.; Mazzella, V.; et al. New Imidazolium Alkaloids with Broad Spectrum of Action from the Marine Bacterium Shewanella Aquimarina. *Pharmaceutics* **2023**, *15*, 2139. [CrossRef] [PubMed]
16. Ng, I.-S.; Ye, C.; Zhang, Z.; Lu, Y.; Jing, K. Daptomycin Antibiotic Production Processes in Fed-Batch Fermentation by Streptomyces Roseosporus NRRL11379 with Precursor Effect and Medium Optimization. *Bioprocess. Biosyst. Eng.* **2014**, *37*, 415–423. [CrossRef] [PubMed]
17. Rimal, B.; Chang, J.; Liu, C.; Rashid, R.; Singh, M.; Kim, S.J. The Effects of Daptomycin on Cell Wall Biosynthesis in Enterococcal Faecalis. *Sci. Rep.* **2023**, *13*, 12227. [CrossRef]
18. Alonzo, D.A.; Schmeing, T.M. Biosynthesis of Depsipeptides, or Depsi: The Peptides with Varied Generations. *Protein Sci.* **2020**, *29*, 2316–2347. [CrossRef]
19. Zeng, M.; Tao, J.; Xu, S.; Bai, X.; Zhang, H. Marine Organisms as a Prolific Source of Bioactive Depsipeptides. *Mar. Drugs* **2023**, *21*, 120. [CrossRef] [PubMed]
20. Sayyed, R.Z.; El-Enshasy, H.A.; Hameeda, B. *Microbial Surfactants: Volume I: Production and Applications*; CRC Press: Boca Raton, FL, USA, 2021; ISBN 978-1-00-041565-0.
21. Haque, E.; Kayalvizhi, K.; Hassan, S. Biocompatibility, Antioxidant and Anti-Infective Effect of Biosurfactant Produced by Marinobacter Litoralis MB15. *Int. J. Pharm. Investig.* **2020**, *10*, 173–178. [CrossRef]
22. Kumar, A.; Singh, S.K.; Kant, C.; Verma, H.; Kumar, D.; Singh, P.P.; Modi, A.; Droby, S.; Kesawat, M.S.; Alavilli, H.; et al. Microbial Biosurfactant: A New Frontier for Sustainable Agriculture and Pharmaceutical Industries. *Antioxidants* **2021**, *10*, 1472. [CrossRef]
23. Rofeal, M.; El-Malek, F.A. Valorization of Lipopeptides Biosurfactants as Anticancer Agents. *Int. J. Pept. Res. Ther.* **2021**, *27*, 447–455. [CrossRef]
24. Giugliano, R.; Buonocore, C.; Zannella, C.; Chianese, A.; Palma Esposito, F.; Tedesco, P.; De Filippis, A.; Galdiero, M.; Franci, G.; de Pascale, D. Antiviral Activity of the Rhamnolipids Mixture from the Antarctic Bacterium Pseudomonas Gessardii M15 against Herpes Simplex Viruses and Coronaviruses. *Pharmaceutics* **2021**, *13*, 2121. [CrossRef] [PubMed]
25. Buonocore, C.; Giugliano, R.; Della Sala, G.; Palma Esposito, F.; Tedesco, P.; Folliero, V.; Galdiero, M.; Franci, G.; de Pascale, D. Evaluation of Antimicrobial Properties and Potential Applications of Pseudomonas Gessardii M15 Rhamnolipids towards Multiresistant Staphylococcus Aureus. *Pharmaceutics* **2023**, *15*, 700. [CrossRef]
26. Xiao, S.; Chen, N.; Chai, Z.; Zhou, M.; Xiao, C.; Zhao, S.; Yang, X. Secondary Metabolites from Marine-Derived Bacillus: A Comprehensive Review of Origins, Structures, and Bioactivities. *Mar. Drugs* **2022**, *20*, 567. [CrossRef]
27. Ali, N.; Pang, Z.; Wang, F.; Xu, B.; El-Seedi, H.R. Lipopeptide Biosurfactants from *Bacillus* spp.: Types, Production, Biological Activities, and Applications in Food. *J. Food Qual.* **2022**, *2022*, 3930112. [CrossRef]
28. Huang, L.; Ling, X.; Peng, S.; Tan, M.; Yan, L.; Liang, Y.; Li, G.; Li, K. A Marine Lipopeptides-Producing Bacillus Amyloliquefaciens HY2-1 with a Broad-Spectrum Antifungal and Antibacterial Activity and Its Fermentation Kinetics Study. *World J. Microbiol. Biotechnol.* **2023**, *39*, 196. [CrossRef] [PubMed]
29. Süssmuth, R.D.; Mainz, A. Nonribosomal Peptide Synthesis-Principles and Prospects. *Angew. Chem. Int. Ed. Engl.* **2017**, *56*, 3770–3821. [CrossRef]
30. Agrawal, S.; Acharya, D.; Adholeya, A.; Barrow, C.J.; Deshmukh, S.K. Nonribosomal Peptides from Marine Microbes and Their Antimicrobial and Anticancer Potential. *Front. Pharmacol.* **2017**, *8*, 828. [CrossRef] [PubMed]
31. Fouillaud, M.; Dufossé, L. Microbial Secondary Metabolism and Biotechnology. *Microorganisms* **2022**, *10*, 123. [CrossRef] [PubMed]
32. Strieker, M.; Tanović, A.; Marahiel, M.A. Nonribosomal Peptide Synthetases: Structures and Dynamics. *Curr. Opin. Struct. Biol.* **2010**, *20*, 234–240. [CrossRef] [PubMed]
33. Shoji, J.; Hinoo, H.; Wakisaka, Y.; Koizumi, K.; Mayama, M. Isolation of a New Peptide Antibiotic TL-119. Studies on Antibiotics from the Genus Bacillus. IV. *J. Antibiot.* **1975**, *28*, 126–128. [CrossRef]
34. Nakagawa, Y.; Nakazawa, T.; Shoji, J. On the Structure of a New Antibiotic TL-119 (Studies on Antibiotics from the Genus Bacillus. VI). *J. Antibiot.* **1975**, *28*, 1004–1005. [CrossRef]
35. Kitajima, Y.; Waki, M.; Shoji, J.; Ueno, T.; Izumiya, N. Revised Structure of the Peptide Lactone Antibiotic, TL-119 and/or A-3302-B. *FEBS Lett.* **1990**, *270*, 139–142. [CrossRef]
36. Sureram, S.; Arduino, I.; Ueoka, R.; Rittà, M.; Francese, R.; Srivibool, R.; Darshana, D.; Piel, J.; Ruchirawat, S.; Muratori, L.; et al. The Peptide A-3302-B Isolated from a Marine Bacterium *Micromonospora* sp. Inhibits HSV-2 Infection by Preventing the Viral Egress from Host Cells. *Int. J. Mol. Sci.* **2022**, *23*, 947. [CrossRef] [PubMed]

37. Lin, Z.; Reilly, C.A.; Antemano, R.; Hughen, R.W.; Marett, L.; Concepcion, G.P.; Haygood, M.G.; Olivera, B.M.; Light, A.; Schmidt, E.W. Nobilamides A–H, Long-Acting Transient Receptor Potential Vanilloid-1 (TRPV1) Antagonists from Mollusk-Associated Bacteria. *J. Med. Chem.* **2011**, *54*, 3746–3755. [CrossRef]
38. Chen, X.; Lu, Y.; Shan, M.; Zhao, H.; Lu, Z.; Lu, Y. A Mini-Review: Mechanism of Antimicrobial Action and Application of Surfactin. *World J. Microbiol. Biotechnol.* **2022**, *38*, 143. [CrossRef] [PubMed]
39. Holder, I.A.; Boyce, S.T. Agar Well Diffusion Assay Testing of Bacterial Susceptibility to Various Antimicrobials in Concentrations Non-Toxic for Human Cells in Culture. *Burns* **1994**, *20*, 426–429. [CrossRef] [PubMed]
40. Khan, H.A.; Baig, F.K.; Mehboob, R. Nosocomial Infections: Epidemiology, Prevention, Control and Surveillance. *Asian Pac. J. Trop. Biomed.* **2017**, *7*, 478–482. [CrossRef]
41. Ashfaq, M.; Talreja, N.; Chauhan, D.; Viswanathan, M.R. Synthesis of Cu-Doped 2D-WS2 Nanosheet-Based Nano-Antibiotic Materials for Inhibiting E. Coli and S. Aureus Bacterial Strains. *New J. Chem.* **2022**, *46*, 5581–5587. [CrossRef]
42. O'Connor, E.; Hynes, S.; Chen, W. Estimating the Non-Market Benefit Value of Deep-Sea Ecosystem Restoration: Evidence from a Contingent Valuation Study of the Dohrn Canyon in the Bay of Naples. *J. Environ. Manag.* **2020**, *275*, 111180. [CrossRef] [PubMed]
43. Della Sala, G.; Mangoni, A.; Costantino, V.; Teta, R. Identification of the Biosynthetic Gene Cluster of Thermoactinoamides and Discovery of New Congeners by Integrated Genome Mining and MS-Based Molecular Networking. *Front. Chem.* **2020**, *8*, 397. [CrossRef] [PubMed]
44. Teta, R.; Sala, G.D.; Esposito, G.; Stornaiuolo, M.; Scarpato, S.; Casazza, M.; Anastasio, A.; Lega, M.; Costantino, V. Monitoring Cyanobacterial Blooms during the COVID-19 Pandemic in Campania, Italy: The Case of Lake Avernus. *Toxins* **2021**, *13*, 471. [CrossRef] [PubMed]
45. Théatre, A.; Cano-Prieto, C.; Bartolini, M.; Laurin, Y.; Deleu, M.; Niehren, J.; Fida, T.; Gerbinet, S.; Alanjary, M.; Medema, M.H.; et al. The Surfactin-Like Lipopeptides From *Bacillus* spp.: Natural Biodiversity and Synthetic Biology for a Broader Application Range. *Front. Bioeng. Biotechnol.* **2021**, *9*, 623701. [CrossRef] [PubMed]
46. Zhen, C.; Ge, X.-F.; Lu, Y.-T.; Liu, W.-Z. Chemical Structure, Properties and Potential Applications of Surfactin, as Well as Advanced Strategies for Improving Its Microbial Production. *AIMS Microbiol.* **2023**, *9*, 195. [CrossRef]
47. Iloabuchi, K.; Spiteller, D. The Epiphyte *Bacillus* sp. G2112 Produces a Large Diversity of Nobilamide Peptides That Promote Biofilm Formation in Pseudomonads and Mycobacterium Aurum. *Biomolecules* **2024**, *14*, 1244. [CrossRef]
48. Medzihradszky, K.F.; Chalkley, R.J. Lessons in de Novo Peptide Sequencing by Tandem Mass Spectrometry. *Mass Spectrom. Rev.* **2015**, *34*, 43–63. [CrossRef]
49. Magarvey, N.A.; Ehling-Schulz, M.; Walsh, C.T. Characterization of the Cereulide NRPS α-Hydroxy Acid Specifying Modules: Activation of α-Keto Acids and Chiral Reduction on the Assembly Line. *J. Am. Chem. Soc.* **2006**, *128*, 10698–10699. [CrossRef] [PubMed]
50. Wenzel, S.C.; Müller, R. Formation of Novel Secondary Metabolites by Bacterial Multimodular Assembly Lines: Deviations from Textbook Biosynthetic Logic. *Curr. Opin. Chem. Biol.* **2005**, *9*, 447–458. [CrossRef] [PubMed]
51. Wenzel, S.C.; Meiser, P.; Binz, T.M.; Mahmud, T.; Müller, R. Nonribosomal Peptide Biosynthesis: Point Mutations and Module Skipping Lead to Chemical Diversity. *Angew. Chem. Int. Ed.* **2006**, *45*, 2296–2301. [CrossRef] [PubMed]
52. Wang, L.; Linares-Otoya, V.; Liu, Y.; Mettal, U.; Marner, M.; Armas-Mantilla, L.; Willbold, S.; Kurtán, T.; Linares-Otoya, L.; Schäberle, T.F. Discovery and Biosynthesis of Antimicrobial Phenethylamine Alkaloids from the Marine Flavobacterium Tenacibaculum Discolor Sv11. *J. Nat. Prod.* **2022**, *85*, 1039–1051. [CrossRef] [PubMed]
53. Shen, Q.; Zhou, H.; Dai, G.; Zhong, G.; Huo, L.; Li, A.; Liu, Y.; Yang, M.; Ravichandran, V.; Zheng, Z.; et al. Characterization of a Cryptic NRPS Gene Cluster in Bacillus Velezensis FZB42 Reveals a Discrete Oxidase Involved in Multithiazole Biosynthesis. *ACS Catal.* **2022**, *12*, 3371–3381. [CrossRef]
54. Baars, O.; Zhang, X.; Gibson, M.I.; Stone, A.T.; Morel, F.M.M.; Seyedsayamdost, M.R. Crochelins: Siderophores with an Unprecedented Iron-Chelating Moiety from the Nitrogen-Fixing Bacterium Azotobacter Chroococcum. *Angew. Chem. Int. Ed.* **2018**, *57*, 536–541. [CrossRef] [PubMed]
55. Chen, H.; Zhong, L.; Zhou, H.; Bai, X.; Sun, T.; Wang, X.; Zhao, Y.; Ji, X.; Tu, Q.; Zhang, Y.; et al. Biosynthesis and Engineering of the Nonribosomal Peptides with a C-Terminal Putrescine. *Nat. Commun.* **2023**, *14*, 6619. [CrossRef] [PubMed]
56. Gardete, S.; Tomasz, A. Mechanisms of Vancomycin Resistance in Staphylococcus Aureus. *J. Clin. Investig.* **2014**, *124*, 2836–2840. [CrossRef]
57. Kapoor, G.; Saigal, S.; Elongavan, A. Action and Resistance Mechanisms of Antibiotics: A Guide for Clinicians. *J. Anaesthesiol. Clin. Pharmacol.* **2017**, *33*, 300–305. [CrossRef] [PubMed]
58. Yoon, S.-H.; Ha, S.-M.; Kwon, S.; Lim, J.; Kim, Y.; Seo, H.; Chun, J. Introducing EzBioCloud: A Taxonomically United Database of 16S rRNA Gene Sequences and Whole-Genome Assemblies. *Int. J. Syst. Evol. Microbiol.* **2017**, *67*, 1613–1617. [CrossRef] [PubMed]
59. Chalita, M.; Kim, Y.O.; Park, S.; Oh, H.-S.; Cho, J.H.; Moon, J.; Baek, N.; Moon, C.; Lee, K.; Yang, J.; et al. EzBioCloud: A Genome-Driven Database and Platform for Microbiome Identification and Discovery. *Int. J. Syst. Evol. Microbiol.* **2024**, *74*, 006421. [CrossRef] [PubMed]

60. Zhang, Z.; Yin, L.; Li, X.; Zhang, C.; Liu, C.; Wu, Z. The Complete Genome Sequence of Bacillus Halotolerans ZB201702 Isolated from a Drought- and Salt-Stressed Rhizosphere Soil. *Microb. Pathog.* **2018**, *123*, 246–249. [CrossRef]
61. Wu, X.; Wu, H.; Wang, R.; Wang, Z.; Zhang, Y.; Gu, Q.; Farzand, A.; Yang, X.; Semenov, M.; Borriss, R.; et al. Genomic Features and Molecular Function of a Novel Stress-Tolerant Bacillus Halotolerans Strain Isolated from an Extreme Environment. *Biology* **2021**, *10*, 1030. [CrossRef] [PubMed]
62. Blin, K.; Shaw, S.; Augustijn, H.E.; Reitz, Z.L.; Biermann, F.; Alanjary, M.; Fetter, A.; Terlouw, B.R.; Metcalf, W.W.; Helfrich, E.J.N.; et al. antiSMASH 7.0: New and Improved Predictions for Detection, Regulation, Chemical Structures and Visualisation. *Nucleic Acids Res.* **2023**, *51*, W46–W50. [CrossRef] [PubMed]
63. Patteson, J.B.; Fortinez, C.M.; Putz, A.T.; Rodriguez-Rivas, J.; Bryant, L.H.I.; Adhikari, K.; Weigt, M.; Schmeing, T.M.; Li, B. Structure and Function of a Dehydrating Condensation Domain in Nonribosomal Peptide Biosynthesis. *J. Am. Chem. Soc.* **2022**, *144*, 14057–14070. [CrossRef] [PubMed]
64. Ziemert, N.; Podell, S.; Penn, K.; Badger, J.H.; Allen, E.; Jensen, P.R. The Natural Product Domain Seeker NaPDoS: A Phylogeny Based Bioinformatic Tool to Classify Secondary Metabolite Gene Diversity. *PLoS ONE* **2012**, *7*, e34064. [CrossRef] [PubMed]
65. Grundmann, F.; Kaiser, M.; Schiell, M.; Batzer, A.; Kurz, M.; Thanwisai, A.; Chantratita, N.; Bode, H.B. Antiparasitic Chaiyaphumines from Entomopathogenic *Xenorhabdus* sp. PB61.4. *J. Nat. Prod.* **2014**, *77*, 779–783. [CrossRef] [PubMed]
66. Lukat, P.; Katsuyama, Y.; Wenzel, S.; Binz, T.; König, C.; Blankenfeldt, W.; Brönstrup, M.; Müller, R. Biosynthesis of Methyl-Proline Containing Griselimycins, Natural Products with Anti-Tuberculosis Activity. *Chem. Sci.* **2017**, *8*, 7521–7527. [CrossRef] [PubMed]
67. Niehs, S.P.; Dose, B.; Scherlach, K.; Roth, M.; Hertweck, C. Genomics-Driven Discovery of a Symbiont-Specific Cyclopeptide from Bacteria Residing in the Rice Seedling Blight Fungus. *ChemBioChem* **2018**, *19*, 2167–2172. [CrossRef] [PubMed]
68. Ragozzino, C.; Palma Esposito, F.; Buonocore, C.; Tedesco, P.; Coppola, D.; Paccagnella, D.; Ziemert, N.; Della Sala, G.; de de Pascale, D. Integrated Genome and Metabolome Mining Unveiled Structure and Biosynthesis of Novel Lipopeptides from a Deep-sea Rhodococcus. *Microb. Biotechnol.* **2024**, *17*, e70011. [CrossRef] [PubMed]
69. Weisburg, W.G.; Barns, S.M.; Pelletier, D.A.; Lane, D.J. 16S Ribosomal DNA Amplification for Phylogenetic Study. *J. Bacteriol.* **1991**, *173*, 697–703. [CrossRef] [PubMed]
70. Palma Esposito, F.; Giugliano, R.; Della Sala, G.; Vitale, G.A.; Buonocore, C.; Ausuri, J.; Galasso, C.; Coppola, D.; Franci, G.; Galdiero, M.; et al. Combining OSMAC Approach and Untargeted Metabolomics for the Identification of New Glycolipids with Potent Antiviral Activity Produced by a Marine Rhodococcus. *Int. J. Mol. Sci.* **2021**, *22*, 9055. [CrossRef] [PubMed]
71. Wang, M.; Carver, J.J.; Phelan, V.V.; Sanchez, L.M.; Garg, N.; Peng, Y.; Nguyen, D.D.; Watrous, J.; Kapono, C.A.; Luzzatto-Knaan, T.; et al. Sharing and Community Curation of Mass Spectrometry Data with Global Natural Products Social Molecular Networking. *Nat. Biotechnol.* **2016**, *34*, 828–837. [CrossRef] [PubMed]
72. Nothias, L.-F.; Petras, D.; Schmid, R.; Dührkop, K.; Rainer, J.; Sarvepalli, A.; Protsyuk, I.; Ernst, M.; Tsugawa, H.; Fleischauer, M.; et al. Feature-Based Molecular Networking in the GNPS Analysis Environment. *Nat. Methods* **2020**, *17*, 905–908. [CrossRef]
73. Siegmund, I.; Wagner, F. New Method for Detecting Rhamnolipids Excreted byPseudomonas Species during Growth on Mineral Agar. *Biotechnol. Tech.* **1991**, *5*, 265–268. [CrossRef]
74. Morikawa, M.; Hirata, Y.; Imanaka, T. A Study on the Structure–Function Relationship of Lipopeptide Biosurfactants. *Biochim. Biophys. Acta (BBA)—Mol. Cell Biol. Lipids* **2000**, *1488*, 211–218. [CrossRef]
75. Balouiri, M.; Sadiki, M.; Ibnsouda, S.K. Methods for in Vitro Evaluating Antimicrobial Activity: A Review. *J. Pharm. Anal.* **2016**, *6*, 71–79. [CrossRef] [PubMed]
76. Franci, G.; Folliero, V.; Cammarota, M.; Zannella, C.; Sarno, F.; Schiraldi, C.; de Lera, A.R.; Altucci, L.; Galdiero, M. Epigenetic Modulator UVI5008 Inhibits MRSA by Interfering with Bacterial Gyrase. *Sci. Rep.* **2018**, *8*, 13117. [CrossRef] [PubMed]
77. Dordet-Frisoni, E.; Dorchies, G.; De Araujo, C.; Talon, R.; Leroy, S. Genomic Diversity in Staphylococcus Xylosus. *Appl. Environ. Microbiol.* **2007**, *73*, 7199–7209. [CrossRef] [PubMed]
78. Weinstein, M.P.; Patel, J.B. *Methods for Dilution Antimicrobial Susceptibility Tests for Bacteria That Grow Aerobically: M07-A11*, 11th ed.; Documents/Clinical and Laboratory Standards Institute; Committee for Clinical Laboratory Standards: Wayne, PA, USA, 2018; ISBN 978-1-56238-836-2.
79. Osek, J.; Lachtara, B.; Wieczorek, K. Listeria Monocytogenes—How This Pathogen Survives in Food-Production Environments? *Front. Microbiol.* **2022**, *13*, 866462. [CrossRef]
80. Bolger, A.M.; Lohse, M.; Usadel, B. Trimmomatic: A Flexible Trimmer for Illumina Sequence Data. *Bioinformatics* **2014**, *30*, 2114–2120. [CrossRef] [PubMed]
81. Babraham Bioinformatics—FastQC A Quality Control Tool for High Throughput Sequence Data. Available online: https://www.bioinformatics.babraham.ac.uk/projects/fastqc/ (accessed on 11 July 2024).
82. Li, D.; Liu, C.-M.; Luo, R.; Sadakane, K.; Lam, T.-W. MEGAHIT: An Ultra-Fast Single-Node Solution for Large and Complex Metagenomics Assembly via Succinct de Bruijn Graph. *Bioinformatics* **2015**, *31*, 1674–1676. [CrossRef]
83. Wang, Y.; Zhao, Y.; Bollas, A.; Wang, Y.; Au, K.F. Nanopore Sequencing Technology, Bioinformatics and Applications. *Nat. Biotechnol.* **2021**, *39*, 1348–1365. [CrossRef] [PubMed]

84. Wick, R.R.; Judd, L.M.; Gorrie, C.L.; Holt, K.E. Unicycler: Resolving Bacterial Genome Assemblies from Short and Long Sequencing Reads. *PLoS Comput. Biol.* **2017**, *13*, e1005595. [CrossRef] [PubMed]
85. Bankevich, A.; Nurk, S.; Antipov, D.; Gurevich, A.A.; Dvorkin, M.; Kulikov, A.S.; Lesin, V.M.; Nikolenko, S.I.; Pham, S.; Prjibelski, A.D.; et al. SPAdes: A New Genome Assembly Algorithm and Its Applications to Single-Cell Sequencing. *J. Comput. Biol.* **2012**, *19*, 455–477. [CrossRef] [PubMed]